Effects of time-reversal symmetry violation in quantum graphs

Pavel Exner

Doppler Institute

for Mathematical Physics and Applied Mathematics

Prague

In collaboration with Ram Band, Divya Goel, Jonathan Rohleder and Aviya Strauss

A talk at the conference Operator theory, analysis and mathematical physics

Stockholm University, June 22, 2026

Quantum graphs in a nutshell

The main character of the story needs no extensive introduction here:

- Discoreved by Linus Pauling in 1936 and then forgotten

Quantum graphs in a nutshell

The main character of the story needs no extensive introduction here:

- Discoreved by Linus Pauling in 1936 and then forgotten
- Rediscovered in the 1980s and flourishing since then

Quantum graphs in a nutshell

The main character of the story needs no extensive introduction here:

- Discoreved by Linus Pauling in 1936 and then forgotten
- Rediscovered in the 1980s and flourishing since then
- Most often one analyzes *Schrödinger* and *Dirac operators* on metric graphs used to model *nanostructures* of various types

Quantum graphs in a nutshell

The main character of the story needs no extensive introduction here:

- Discoreved by Linus Pauling in 1936 and then forgotten
- Rediscovered in the 1980s and flourishing since then
- Most often one analyzes *Schrödinger* and *Dirac operators* on metric graphs used to model *nanostructures* of various types
- In addition, *other operators* (higher order, nonlinear, random) as well as *other applications* (waves, elasticity, networks of microwave cables, quantum chaos effects) are of interest

Quantum graphs in a nutshell

The main character of the story needs no extensive introduction here:

- Discoreved by Linus Pauling in 1936 and then forgotten
- Rediscovered in the 1980s and flourishing since then
- Most often one analyzes *Schrödinger* and *Dirac operators* on metric graphs used to model *nanostructures* of various types
- In addition, *other operators* (higher order, nonlinear, random) as well as *other applications* (waves, elasticity, networks of microwave cables, quantum chaos effects) are of interest
- The graph literature is extensive indeed; the best source I can recommend to start with are the monographs

Y.V. Pokornyi, O.M. Penkin, V.L. Pryadiev, A.V. Borovskikh, P.P. Lazarev, S.A. Shabrov: Differential equations on geometric graphs, Fizmatlit, Moscow 2005.

G. Berkolaiko, P. Kuchment: *Introduction to Quantum Graphs*, AMS, Providence, R.I., 2013.

A. Kostenko, N. Nicolussi: *Laplacians on Infinite Graphs*, Mem. EMS, Berlin 2022.

P. Kurasov: *Spectral Geometry of Graphs*, Birkhäuser, Berlin 2024.

Vertex coupling in quantum graphs

Often reduced to the simplest case, but it is a crucial ingredient.

Vertex coupling in quantum graphs

Often reduced to the simplest case, but it is a crucial ingredient.

The boundary values being written as columns, $\psi(0) := \{\psi_j(0)\}$ and $\psi'(0) := \{\psi'_j(0)\}$, understood as left limits at the endpoint; then the most general self-adjoint matching conditions are of the form

$$A\psi(0) + B\psi'(0) = 0,$$

where the $n \times n$ matrices A, B satisfy the conditions

- $\mathrm{rank}\,(A, B) = n$

Vertex coupling in quantum graphs

Often reduced to the simplest case, but it is a crucial ingredient.

The boundary values being written as columns, $\psi(0) := \{\psi_j(0)\}$ and $\psi'(0) := \{\psi_j'(0)\}$, understood as left limits at the endpoint; then the most general self-adjoint matching conditions are of the form

$$A\psi(0) + B\psi'(0) = 0,$$

where the $n \times n$ matrices A, B satisfy the conditions

- $\mathrm{rank}\,(A, B) = n$
- AB^* is *Hermitean*

V. Kostrykin, R. Schrader: Kirhhoff's rule for quantum wires, *J. Phys. A: Math. Gen.* **32** (1999), 595–630.

Vertex coupling in quantum graphs

Often reduced to the simplest case, but it is a crucial ingredient.

The boundary values being written as columns, $\psi(0) := \{\psi_j(0)\}$ and $\psi'(0) := \{\psi_j'(0)\}$, understood as left limits at the endpoint; then the most general self-adjoint matching conditions are of the form

$$A\psi(0) + B\psi'(0) = 0,$$

where the $n \times n$ matrices A, B satisfy the conditions

- $\mathrm{rank}\,(A, B) = n$
- AB^* is *Hermitean*

V. Kostrykin, R. Schrader: Kirhhoff's rule for quantum wires, *J. Phys. A: Math. Gen.* **32** (1999), 595–630.

F.S.Rofe-Beketov: Self-adjoint extensions of differential operators in a space of vector-valued functions, *Teor. Funkcii, Funkcional. Anal. Prilozh.* **8** (1969), 3–24 (in Russian).

Vertex coupling in quantum graphs

Often reduced to the simplest case, but it is a crucial ingredient.

The boundary values being written as columns, $\psi(0) := \{\psi_j(0)\}$ and $\psi'(0) := \{\psi'_j(0)\}$, understood as left limits at the endpoint; then the most general self-adjoint matching conditions are of the form

$$A\psi(0) + B\psi'(0) = 0,$$

where the $n \times n$ matrices A, B satisfy the conditions

- $\mathrm{rank}\,(A, B) = n$
- AB^* is *Hermitean*

V. Kostrykin, R. Schrader: Kirhhoff's rule for quantum wires, *J. Phys. A: Math. Gen.* **32** (1999), 595–630.

F.S.Rofe-Beketov: Self-adjoint extensions of differential operators in a space of vector-valued functions, *Teor. Funkcii, Funkcional. Anal. Prilozh.* **8** (1969), 3–24 (in Russian).

Naturally, these conditions are non-unique, as A, B can be replaced by CA, CB with a *regular* C. This non-uniqueness can be removed by using

$$(U - I)\psi(0) + i\ell(U + I)\psi'(0) = 0,$$

where U is a *unitary* $n \times n$ *matrix*

Vertex coupling in quantum graphs

Often reduced to the simplest case, but it is a crucial ingredient.

The boundary values being written as columns, $\psi(0) := \{\psi_j(0)\}$ and $\psi'(0) := \{\psi'_j(0)\}$, understood as left limits at the endpoint; then the most general self-adjoint matching conditions are of the form

$$A\psi(0) + B\psi'(0) = 0,$$

where the $n \times n$ matrices A, B satisfy the conditions

- $\mathrm{rank}\,(A, B) = n$
- AB^* is *Hermitean*

V. Kostrykin, R. Schrader: Kirhhoff's rule for quantum wires, *J. Phys. A: Math. Gen.* **32** (1999), 595–630.

F.S.Rofe-Beketov: Self-adjoint extensions of differential operators in a space of vector-valued functions, *Teor. Funkcii, Funkcional. Anal. Prilozh.* **8** (1969), 3–24 (in Russian).

Naturally, these conditions are non-unique, as A, B can be replaced by CA, CB with a *regular* C. This non-uniqueness can be removed by using

$$(U - I)\psi(0) + i\ell(U + I)\psi'(0) = 0,$$

where U is a *unitary $n \times n$ matrix* (usually we fix the length scale choosing $\ell = 1$).

(A)symmetry of the vertex coupling

Many vertex coupling are time-reversal symmetric, e.g., the δ-coupling,

$$\psi_j(0) = \psi_k(0) = \psi(0) \;\text{ for } j,k = 1,\dots,n, \quad \sum_{j=1}^{n} \psi_j'(0) = \alpha\psi(0)\,;$$

recall that the simplest case $\alpha = 0$, is usually called *(Neumann-)Kirchhoff*.

(A)symmetry of the vertex coupling

Many vertex coupling are time-reversal symmetric, e.g., the δ-coupling,

$$\psi_j(0) = \psi_k(0) = \psi(0) \text{ for } j,k = 1,\dots,n, \quad \sum_{j=1}^{n} \psi_j'(0) = \alpha\psi(0)\,;$$

recall that the simplest case $\alpha = 0$, is usually called *(Neumann-)Kirchhoff*.

However, those violating the invariance may be of interest. Motivated by attempts to model the *anomalous Hall effect*, we started looking into

$$U = R, \text{ where } R_{ij} = \delta_{i,i+1} \pmod{n},$$

which refers to *'maximum violation'* at $k = \ell^{-1}$

(A)symmetry of the vertex coupling

Many vertex coupling are time-reversal symmetric, e.g., the δ-coupling,

$$\psi_j(0) = \psi_k(0) = \psi(0) \text{ for } j, k = 1, \dots, n, \quad \sum_{j=1}^{n} \psi_j'(0) = \alpha\psi(0)\,;$$

recall that the simplest case $\alpha = 0$, is usually called *(Neumann-)Kirchhoff*.

However, those violating the invariance may be of interest. Motivated by attempts to model the *anomalous Hall effect*, we started looking into

$$U = R, \text{ where } R_{ij} = \delta_{i,j+1} \pmod{n},$$

which refers to *'maximum violation'* at $k = \ell^{-1}$; recall that the *on-shell S-matrix* at momentum k is $S(k) = \frac{k\ell-1+(k\ell+1)U}{k\ell+1+(k\ell-1)U}$ so that $S(\ell^{-1}) = U$

(A)symmetry of the vertex coupling

Many vertex coupling are time-reversal symmetric, e.g., the δ-coupling,

$$\psi_j(0) = \psi_k(0) = \psi(0) \text{ for } j,k = 1,\dots,n, \quad \sum_{j=1}^{n} \psi_j'(0) = \alpha\psi(0)\,;$$

recall that the simplest case $\alpha = 0$, is usually called *(Neumann-)Kirchhoff*.

However, those violating the invariance may be of interest. Motivated by attempts to model the *anomalous Hall effect*, we started looking into

$$U = R, \text{ where } R_{ij} = \delta_{i,j+1} \pmod n,$$

which refers to *'maximum violation'* at $k = \ell^{-1}$; recall that the *on-shell S-matrix* at momentum k is $S(k) = \frac{k\ell - 1 + (k\ell+1)U}{k\ell+1+(k\ell-1)U}$ so that $S(\ell^{-1}) = U$

Writing this coupling componentwise for vertex of degree n, we have

$$(\psi_{j+1} - \psi_j) + i\ell(\psi_{j+1}' + \psi_j') = 0\,, \quad j \in \mathbb{Z} \pmod n\,,$$

non-trivial for $n \geq 3$ and non-invariant w.r.t. the *complex conjugation*.

(A)symmetry condition

One naturally asks how can be time (a)symmetric characterized. A straightforward answer is that time-reversal symmetry requires the possibility to choose the matrix coefficients A, B in the vertex condition *real-valued*

(A)symmetry condition

One naturally asks how can be time (a)symmetric characterized. A straightforward answer is that time-reversal symmetry requires the possibility to choose the matrix coefficients A, B in the vertex condition *real-valued*. As mentioned, though, they are non-unique so one would prefer expression the (a)symmetry in terms of the matrix U.

(A)symmetry condition

One naturally asks how can be time (a)symmetric characterized. A straightforward answer is that time-reversal symmetry requires the possibility to choose the matrix coefficients A, B in the vertex condition *real-valued*. As mentioned, though, they are non-unique so one would prefer expression the (a)symmetry in terms of the matrix U.

We are interested in symmetries associated with the vertices: each one is associated with an invertible map in the space of the boundary values, $\Theta : \mathbb{C}^n \to \mathbb{C}^n$, such that we have $(U - I)\Theta\psi(0) + i(U + I)\Theta\psi'(0) = 0$ for all admissible ψ, or $\Theta^{-1}U\Theta = U$.

(A)symmetry condition

One naturally asks how can be time (a)symmetric characterized. A straightforward answer is that time-reversal symmetry requires the possibility to choose the matrix coefficients A, B in the vertex condition *real-valued*. As mentioned, though, they are non-unique so one would prefer expression the (a)symmetry in terms of the matrix U.

We are interested in symmetries associated with the vertices: each one is associated with an invertible map in the space of the boundary values, $\Theta : \mathbb{C}^n \to \mathbb{C}^n$, such that we have $(U-I)\Theta\psi(0) + i(U+I)\Theta\psi'(0) = 0$ for all admissible ψ, or $\Theta^{-1}U\Theta = U$.

The time reversal map $\Theta_{\mathcal{T}}$ is *antilinear* and *idempotent*, in the absence of internal degrees of freedom it is just the *complex conjugation*. The unitarity, $U^T\bar{U} = \bar{U}U^T = I$, means that $\bar{\psi}$ satisfies the vertex condition with the *transposed matrix*, that is,

$$\Theta_{\mathcal{T}}^{-1} U \Theta_{\mathcal{T}} = \Theta_{\mathcal{T}} U \Theta_{\mathcal{T}} = U^T,$$

and consequently, the *H_U is $\mathcal{T}$-invariant if and only if* $U = U^T$.

A reminder: circulant matrices

Matrix R belongs to the *circulant class*; let us recall what it is like:

$$U = \begin{pmatrix} c_1 & c_2 & \cdots & c_{n-1} & c_n \\ c_n & c_1 & c_2 & & c_{n-1} \\ \vdots & c_n & c_1 & \ddots & \vdots \\ c_3 & & \ddots & \ddots & c_2 \\ c_2 & c_3 & \cdots & c_n & c_1 \end{pmatrix}.$$

Their eigenvectors $\phi_j = \frac{1}{\sqrt{n}}\left(1, \omega^j, \omega^{2j}, \dots, \omega^{(n-1)j}\right)^T$, $j = 1, \dots, n$, where $\omega := \mathrm{e}^{2\pi i/n}$, are independent of the choice of the c_j's, the diagonalization being achievbed by the *discrete Fourier transformation*,

$$V^* = \frac{1}{\sqrt{n}} \begin{pmatrix} 1 & 1 & 1 & 1 & \dots & 1 \\ 1 & \omega & \omega^2 & \omega^3 & \dots & \omega^{(n-1)} \\ 1 & \omega^2 & \omega^4 & \omega^6 & \dots & \omega^{2(n-1)} \\ \vdots & \vdots & \vdots & \vdots & & \vdots \\ 1 & \omega^{n-1} & \omega^{2(n-1)} & \omega^{3(n-1)} & \dots & \omega^{(n-1)^2} \end{pmatrix}.$$

A reminder: circulant matrices

Matrix R belongs to the *circulant class*; let us recall what it is like:

$$U = \begin{pmatrix} c_1 & c_2 & \cdots & c_{n-1} & c_n \\ c_n & c_1 & c_2 & & c_{n-1} \\ \vdots & c_n & c_1 & \ddots & \vdots \\ c_3 & & \ddots & \ddots & c_2 \\ c_2 & c_3 & \cdots & c_n & c_1 \end{pmatrix}.$$

Their eigenvectors $\phi_j = \frac{1}{\sqrt{n}}\left(1, \omega^j, \omega^{2j}, \dots, \omega^{(n-1)j}\right)^T$, $j = 1, \dots, n$, where $\omega := \mathrm{e}^{2\pi i/n}$, are independent of the choice of the c_j's, the diagonalization being achievbed by the *discrete Fourier transformation*,

$$V^* = \frac{1}{\sqrt{n}} \begin{pmatrix} 1 & 1 & 1 & 1 & \dots & 1 \\ 1 & \omega & \omega^2 & \omega^3 & \dots & \omega^{(n-1)} \\ 1 & \omega^2 & \omega^4 & \omega^6 & \dots & \omega^{2(n-1)} \\ \vdots & \vdots & \vdots & \vdots & & \vdots \\ 1 & \omega^{n-1} & \omega^{2(n-1)} & \omega^{3(n-1)} & \dots & \omega^{(n-1)^2} \end{pmatrix}.$$

The eigenvalues in terms of the matrix entries are $\lambda_j = \sum_{k=1}^n c_k \omega^{j(k-1)}$ and conversely, we have $c_j = \frac{1}{n} \sum_{k=1}^n \lambda_k \omega^{-j(k-1)}$, $j = 1, \dots, n$.

$\mathcal{PT}$-symmetry

Time reversal can be combined with other symmetries. For instance, assuming that the vertex coupling is *circular*, we achieve validity of the relation $\Theta U \Theta = U^T$ choosing the matrix $\Theta = \Theta_{\mathcal{P}}$ of the form

$$\Theta_{\mathcal{P}} = V^T V = \begin{pmatrix} 1 & 0 & 0 & \cdots & 0 & 0 & 0 \\ 0 & 0 & 0 & \cdots & 0 & 0 & 1 \\ 0 & 0 & 0 & \cdots & 0 & 1 & 0 \\ \vdots & & & \iddots & & & \vdots \\ 0 & 0 & 1 & \cdots & 0 & 0 & 0 \\ 0 & 1 & 0 & \cdots & 0 & 0 & 0 \end{pmatrix}$$

which in case of *planar graphs* can be reasonably interpreted as the transformation describing *mirror reflection.*

$\mathcal{PT}$-symmetry

Time reversal can be combined with other symmetries. For instance, assuming that the vertex coupling is *circular*, we achieve validity of the relation $\Theta U \Theta = U^T$ choosing the matrix $\Theta = \Theta_{\mathcal{P}}$ of the form

$$\Theta_{\mathcal{P}} = V^T V = \begin{pmatrix} 1 & 0 & 0 & \cdots & 0 & 0 & 0 \\ 0 & 0 & 0 & \cdots & 0 & 0 & 1 \\ 0 & 0 & 0 & \cdots & 0 & 1 & 0 \\ \vdots & & & \iddots & & & \vdots \\ 0 & 0 & 1 & \cdots & 0 & 0 & 0 \\ 0 & 1 & 0 & \cdots & 0 & 0 & 0 \end{pmatrix}$$

which in case of *planar graphs* can be reasonably interpreted as the transformation describing *mirror reflection.*

Consequently, the n parameter family of *circulant vertex couplings* (out of total n^2 parameters) contains an $\lfloor \frac{n-1}{2} \rfloor$-parameter subset the elements of which exhibit a *nontrivial* $\mathcal{PT}$ while being *self-adjoint.*

P.E., M. Tater: Quantum graphs: self-adjoint, and yet exhibiting a nontrivial $\mathcal{PT}$-symmetry, *Phys. Lett.* **A416** (2021), 127669

$\mathcal{PT}$-symmetry

Time reversal can be combined with other symmetries. For instance, assuming that the vertex coupling is *circular*, we achieve validity of the relation $\Theta U \Theta = U^T$ choosing the matrix $\Theta = \Theta_{\mathcal{P}}$ of the form

$$\Theta_{\mathcal{P}} = V^T V = \begin{pmatrix} 1 & 0 & 0 & \cdots & 0 & 0 & 0 \\ 0 & 0 & 0 & \cdots & 0 & 0 & 1 \\ 0 & 0 & 0 & \cdots & 0 & 1 & 0 \\ \vdots & & & \iddots & & & \vdots \\ 0 & 0 & 1 & \cdots & 0 & 0 & 0 \\ 0 & 1 & 0 & \cdots & 0 & 0 & 0 \end{pmatrix}$$

which in case of *planar graphs* can be reasonably interpreted as the transformation describing *mirror reflection.*

Consequently, the n parameter family of *circulant vertex couplings* (out of total n^2 parameters) contains an $\lfloor \frac{n-1}{2} \rfloor$-parameter subset the elements of which exhibit a *nontrivial $\mathcal{PT}$* while being *self-adjoint.*

P.E., M. Tater: Quantum graphs: self-adjoint, and yet exhibiting a nontrivial $\mathcal{PT}$-symmetry, *Phys. Lett.* **A416** (2021), 127669

After this interlude, let us return to the R coupling.

Stars with R coupling: spectrum and scattering

Consider first a *star graph* with n semi-infinite edges and the above coupling with $\ell = 1$. Obviously, we have $\sigma_{\mathrm{ess}}(H) = \mathbb{R}_+$

Stars with R coupling: spectrum and scattering

Consider first a *star graph* with n semi-infinite edges and the above coupling with $\ell = 1$. Obviously, we have $\sigma_{\mathrm{ess}}(H) = \mathbb{R}_+$. It is also easy to check that H has eigenvalues $-\kappa^2$, where

$$\kappa = \tan \frac{\pi m}{n}$$

with m running through $1, \dots, [\frac{n}{2}]$ for n odd and $1, \dots, [\frac{n-1}{2}]$ for n even. Thus $\sigma_{\mathrm{disc}}(H)$ is *always nonempty*

Stars with R coupling: spectrum and scattering

Consider first a *star graph* with n semi-infinite edges and the above coupling with $\ell = 1$. Obviously, we have $\sigma_{\mathrm{ess}}(H) = \mathbb{R}_+$. It is also easy to check that H has eigenvalues $-\kappa^2$, where

$$\kappa = \tan \frac{\pi m}{n}$$

with m running through $1, \dots, [\frac{n}{2}]$ for n odd and $1, \dots, [\frac{n-1}{2}]$ for n even. Thus $\sigma_{\mathrm{disc}}(H)$ is *always nonempty*, in particular, H has a single negative eigenvalue for $n = 3, 4$ which is equal to -3 and -1, respectively.

Stars with R coupling: spectrum and scattering

Consider first a *star graph* with n semi-infinite edges and the above coupling with $\ell = 1$. Obviously, we have $\sigma_{\mathrm{ess}}(H) = \mathbb{R}_+$. It is also easy to check that H has eigenvalues $-\kappa^2$, where

$$\kappa = \tan \frac{\pi m}{n}$$

with m running through $1, \dots, [\frac{n}{2}]$ for n odd and $1, \dots, [\frac{n-1}{2}]$ for n even. Thus $\sigma_{\mathrm{disc}}(H)$ is *always nonempty*, in particular, H has a single negative eigenvalue for $n = 3, 4$ which is equal to -3 and -1, respectively.

As for the scattering, we know that $S(k) = \frac{k-1+(k+1)U}{k+1+(k-1)U}$. It might seem that transport becomes trivial at small and high energies, since it looks like we have $\lim_{k\to 0} S(k) = -I$ and $\lim_{k\to\infty} S(k) = I$.

Stars with R coupling: spectrum and scattering

Consider first a *star graph* with n semi-infinite edges and the above coupling with $\ell = 1$. Obviously, we have $\sigma_{\mathrm{ess}}(H) = \mathbb{R}_+$. It is also easy to check that H has eigenvalues $-\kappa^2$, where

$$\kappa = \tan \frac{\pi m}{n}$$

with m running through $1, \dots, [\frac{n}{2}]$ for n odd and $1, \dots, [\frac{n-1}{2}]$ for n even. Thus $\sigma_{\mathrm{disc}}(H)$ is *always nonempty*, in particular, H has a single negative eigenvalue for $n = 3, 4$ which is equal to -3 and -1, respectively.

As for the scattering, we know that $S(k) = \frac{k-1+(k+1)U}{k+1+(k-1)U}$. It might seem that transport becomes trivial at small and high energies, since it looks like we have $\lim_{k\to 0} S(k) = -I$ and $\lim_{k\to\infty} S(k) = I$.

However, caution is needed; the formal limits lead to a *false result* if $+1$ or -1 are eigenvalues of U

Stars with R coupling: spectrum and scattering

Consider first a *star graph* with n semi-infinite edges and the above coupling with $\ell = 1$. Obviously, we have $\sigma_{\mathrm{ess}}(H) = \mathbb{R}_+$. It is also easy to check that H has eigenvalues $-\kappa^2$, where

$$\kappa = \tan \frac{\pi m}{n}$$

with m running through $1, \dots, [\frac{n}{2}]$ for n odd and $1, \dots, [\frac{n-1}{2}]$ for n even. Thus $\sigma_{\mathrm{disc}}(H)$ is *always nonempty*, in particular, H has a single negative eigenvalue for $n = 3, 4$ which is equal to -3 and -1, respectively.

As for the scattering, we know that $S(k) = \frac{k-1+(k+1)U}{k+1+(k-1)U}$. It might seem that transport becomes trivial at small and high energies, since it looks like we have $\lim_{k\to 0} S(k) = -I$ and $\lim_{k\to\infty} S(k) = I$.

However, caution is needed; the formal limits lead to a *false result* if $+1$ or -1 are eigenvalues of U. A *counterexample* is the (scale invariant) Kirchhoff coupling where U has only ± 1 as its eigenvalues; the on-shell S-matrix is then independent of k and it is *not* a multiple of the identity.

The S matrix for this coupling

Denoting for simplicity $\eta := \frac{1-k}{1+k}$, a straightforward computation gives

$$S_{ij}(k) = \frac{1-\eta^2}{1-\eta^n} \left\{ -\eta \, \frac{1-\eta^{n-2}}{1-\eta^2} \, \delta_{ij} + (1-\delta_{ij}) \, \eta^{(j-i-1)(\mathrm{mod}\, n)} \right\},$$

The S matrix for this coupling

Denoting for simplicity $\eta := \frac{1-k}{1+k}$, a straightforward computation gives

$$S_{ij}(k) = \frac{1-\eta^2}{1-\eta^n} \left\{ -\eta \, \frac{1-\eta^{n-2}}{1-\eta^2} \, \delta_{ij} + (1-\delta_{ij}) \, \eta^{(j-i-1)(\mathrm{mod}\, n)} \right\},$$

in particular, for $n = 3, 4$, respectively, we get

$$\frac{1+\eta}{1+\eta+\eta^2} \begin{pmatrix} -\frac{\eta}{1+\eta} & 1 & \eta \\ \eta & -\frac{\eta}{1+\eta} & 1 \\ 1 & \eta & -\frac{\eta}{1+\eta} \end{pmatrix} \quad \text{and} \quad \frac{1}{1+\eta^2} \begin{pmatrix} -\eta & 1 & \eta & \eta^2 \\ \eta^2 & -\eta & 1 & \eta \\ \eta & \eta^2 & -\eta & 1 \\ 1 & \eta & \eta^2 & -\eta \end{pmatrix}$$

The S matrix for this coupling

Denoting for simplicity $\eta := \frac{1-k}{1+k}$, a straightforward computation gives

$$S_{ij}(k) = \frac{1-\eta^2}{1-\eta^n} \left\{ -\eta\, \frac{1-\eta^{n-2}}{1-\eta^2}\, \delta_{ij} + (1-\delta_{ij})\, \eta^{(j-i-1) (\mathrm{mod}\, n)} \right\},$$

in particular, for $n = 3, 4$, respectively, we get

$$\frac{1+\eta}{1+\eta+\eta^2} \begin{pmatrix} -\frac{\eta}{1+\eta} & 1 & \eta \\ \eta & -\frac{\eta}{1+\eta} & 1 \\ 1 & \eta & -\frac{\eta}{1+\eta} \end{pmatrix} \quad \text{and} \quad \frac{1}{1+\eta^2} \begin{pmatrix} -\eta & 1 & \eta & \eta^2 \\ \eta^2 & -\eta & 1 & \eta \\ \eta & \eta^2 & -\eta & 1 \\ 1 & \eta & \eta^2 & -\eta \end{pmatrix}$$

We see that $\lim_{k\to\infty} S(k) = I$ holds for $n = 3$ and more generally *for all odd n*, while for the *even ones* the limit is *not a multiple of identity*

The S matrix for this coupling

Denoting for simplicity $\eta := \frac{1-k}{1+k}$, a straightforward computation gives

$$S_{ij}(k) = \frac{1-\eta^2}{1-\eta^n} \left\{ -\eta\, \frac{1-\eta^{n-2}}{1-\eta^2}\, \delta_{ij} + (1-\delta_{ij})\, \eta^{(j-i-1)(\mathrm{mod}\, n)} \right\},$$

in particular, for $n = 3, 4$, respectively, we get

$$\frac{1+\eta}{1+\eta+\eta^2} \begin{pmatrix} -\frac{\eta}{1+\eta} & 1 & \eta \\ \eta & -\frac{\eta}{1+\eta} & 1 \\ 1 & \eta & -\frac{\eta}{1+\eta} \end{pmatrix} \quad \text{and} \quad \frac{1}{1+\eta^2} \begin{pmatrix} -\eta & 1 & \eta & \eta^2 \\ \eta^2 & -\eta & 1 & \eta \\ \eta & \eta^2 & -\eta & 1 \\ 1 & \eta & \eta^2 & -\eta \end{pmatrix}$$

We see that $\lim_{k\to\infty} S(k) = I$ holds for $n = 3$ and more generally *for all odd n*, while for the *even ones* the limit is *not a multiple of identity*. This is is related to the fact that in the latter case U has both ± 1 as its eigenvalues, while for n *odd* -1 is *missing*.

P.E., M. Tater: Quantum graphs with vertices of a preferred orientation, *Phys. Lett.* **A382** (2018), 283–287.

The S matrix for this coupling

Denoting for simplicity $\eta := \frac{1-k}{1+k}$, a straightforward computation gives

$$S_{ij}(k) = \frac{1-\eta^2}{1-\eta^n} \left\{ -\eta\, \frac{1-\eta^{n-2}}{1-\eta^2}\, \delta_{ij} + (1-\delta_{ij})\, \eta^{(j-i-1)(\mathrm{mod}\, n)} \right\},$$

in particular, for $n = 3, 4$, respectively, we get

$$\frac{1+\eta}{1+\eta+\eta^2} \begin{pmatrix} -\frac{\eta}{1+\eta} & 1 & \eta \\ \eta & -\frac{\eta}{1+\eta} & 1 \\ 1 & \eta & -\frac{\eta}{1+\eta} \end{pmatrix} \quad \text{and} \quad \frac{1}{1+\eta^2} \begin{pmatrix} -\eta & 1 & \eta & \eta^2 \\ \eta^2 & -\eta & 1 & \eta \\ \eta & \eta^2 & -\eta & 1 \\ 1 & \eta & \eta^2 & -\eta \end{pmatrix}$$

We see that $\lim_{k\to\infty} S(k) = I$ holds for $n = 3$ and more generally *for all odd n*, while for the *even ones* the limit is *not a multiple of identity*. This is is related to the fact that in the latter case U has both ± 1 as its eigenvalues, while for n *odd* -1 is *missing*.

P.E., M. Tater: Quantum graphs with vertices of a preferred orientation, *Phys. Lett.* **A382** (2018), 283–287.

We will see some consequences of this fact. On the other hand, the association with the vertex parity is specific for this particular coupling.

Spectral properties discussed

Examples of spectra of periodic graphs of various *topologies* such as lattices (rectangular, hexagonal, Kagome, Cairo) or chains

Spectral properties discussed

Examples of spectra of periodic graphs of various *topologies* such as lattices (rectangular, hexagonal, Kagome, Cairo) or chains, and *vertex couplings* such as R, $-R$, or ϵR with $\epsilon \neq i^j$, $j \in \mathbb{Z}$ have been examined.

Spectral properties discussed

Examples of spectra of periodic graphs of various *topologies* such as lattices (rectangular, hexagonal, Kagome, Cairo) or chains, and *vertex couplings* such as R, $-R$, or ϵR with $\epsilon \neq i^j$, $j \in \mathbb{Z}$ have been examined.

I will mention only one example, the *magnetic square lattice* with the R-coupling in which two time-reversal violation *compete*; one finds that at high energies one finds asymptotically the *Hofstadter butterfly pattern*

Spectral properties discussed

Examples of spectra of periodic graphs of various *topologies* such as lattices (rectangular, hexagonal, Kagome, Cairo) or chains, and *vertex couplings* such as R, $-R$, or ϵR with $\epsilon \neq i^j$, $j \in \mathbb{Z}$ have been examined.

I will mention only one example, the *magnetic square lattice* with the R-coupling in which two time-reversal violation *compete*; one finds that at high energies one finds asymptotically the *Hofstadter butterfly pattern*

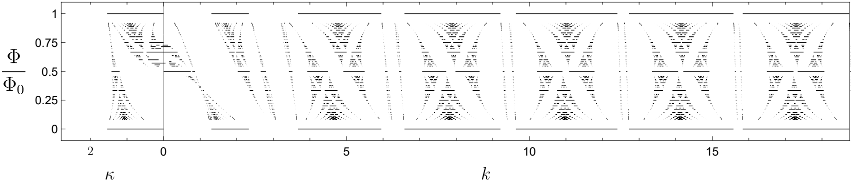

M. Baradaran, P.E., J. Lipovský: Magnetic square lattice with vertex coupling of a preferred orientation, *Ann. Phys.* **454** (2023), 169339

Spectral properties discussed

Examples of spectra of periodic graphs of various *topologies* such as lattices (rectangular, hexagonal, Kagome, Cairo) or chains, and *vertex couplings* such as R, $-R$, or ϵR with $\epsilon \neq i^j$, $j \in \mathbb{Z}$ have been examined.

I will mention only one example, the *magnetic square lattice* with the R-coupling in which two time-reversal violation *compete*; one finds that at high energies one finds asymptotically the *Hofstadter butterfly pattern*

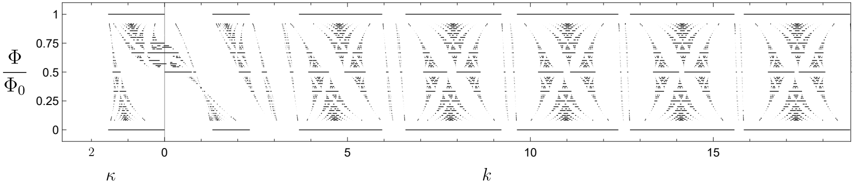

M. Baradaran, P.E., J. Lipovský: Magnetic square lattice with vertex coupling of a preferred orientation, *Ann. Phys.* **454** (2023), 169339

After this introduction, let us turn to our main topic which are spectral properties of *finite graphs with time asymmetric vertex coupling.*

Spectral optimization on graphs with R coupling

Considering general *finite graphs*, let us ask about geometries which optimize the ground state, or more generally, also other eigenvalues.

Spectral optimization on graphs with R coupling

Considering general *finite graphs*, let us ask about geometries which optimize the ground state, or more generally, also other eigenvalues.

As before, we begin with a finite *star graph* Γ with a single vertex v_0 of degree N and edges $e_1, \dots, e_N$ of lengths l_j; we suppose that at the 'loose ends' (if any), *Neumann condition is imposed*.

Spectral optimization on graphs with R coupling

Considering general *finite graphs*, let us ask about geometries which optimize the ground state, or more generally, also other eigenvalues.

As before, we begin with a finite *star graph* Γ with a single vertex v_0 of degree N and edges $e_1, \dots, e_N$ of lengths l_j; we suppose that at the 'loose ends' (if any), *Neumann condition is imposed*.

Using for $f \in \widetilde{H}^k(\Gamma) = \{f : f_j \in H^k(0, l_j), j = 1, \dots, N\}$ the boundary values

$$F = (f_1(0), f_2(0), \dots, f_N(0))^\top \quad \text{and} \quad F' = (f_1'(0), f_2'(0), \dots, f_N'(0))^\top,$$

our operator is as before the (negative) Laplacian with the domain specified by the boundary conditions

$$(F_{j+1} - F_j) + i\left(F_j' + F_{j+1}'\right) = 0, \quad j = 1, \dots, N.$$

Spectral optimization on graphs with R coupling

Considering general *finite graphs*, let us ask about geometries which optimize the ground state, or more generally, also other eigenvalues.

As before, we begin with a finite *star graph* Γ with a single vertex v_0 of degree N and edges $e_1, \dots, e_N$ of lengths l_j; we suppose that at the 'loose ends' (if any), *Neumann condition is imposed*.

Using for $f \in \widetilde{H}^k(\Gamma) = \{f : f_j \in H^k(0, l_j), j = 1, \dots, N\}$ the boundary values

$$F = (f_1(0), f_2(0), \dots, f_N(0))^\top \quad \text{and} \quad F' = (f_1'(0), f_2'(0), \dots, f_N'(0))^\top,$$

our operator is as before the (negative) Laplacian with the domain specified by the boundary conditions

$$(F_{j+1} - F_j) + i\left(F_j' + F_{j+1}'\right) = 0, \quad j = 1, \dots, N.$$

Remarks: Summing over j, we get $\sum_{j=1}^N F_j' = 0$

Spectral optimization on graphs with R coupling

Considering general *finite graphs*, let us ask about geometries which optimize the ground state, or more generally, also other eigenvalues.

As before, we begin with a finite *star graph* Γ with a single vertex v_0 of degree N and edges $e_1, \dots, e_N$ of lengths l_j; we suppose that at the 'loose ends' (if any), *Neumann condition is imposed*.

Using for $f \in \widetilde{H}^k(\Gamma) = \left\{f : f_j \in H^k(0, l_j), j = 1, \dots, N\right\}$ the boundary values

$$F = (f_1(0), f_2(0), \dots, f_N(0))^\top \quad \text{and} \quad F' = (f_1'(0), f_2'(0), \dots, f_N'(0))^\top,$$

our operator is as before the (negative) Laplacian with the domain specified by the boundary conditions

$$(F_{j+1} - F_j) + i\left(F_j' + F_{j+1}'\right) = 0, \quad j = 1, \dots, N.$$

Remarks: Summing over j, we get $\sum_{j=1}^N F_j' = 0$. Moreover, if N is *even*, then summing with $(-1)^j$ leads to the relation $\sum_{j=1}^N F_j = 0$.

Spectral optimization on graphs with R coupling

Considering general *finite graphs*, let us ask about geometries which optimize the ground state, or more generally, also other eigenvalues.

As before, we begin with a finite *star graph* Γ with a single vertex v_0 of degree N and edges $e_1, \dots, e_N$ of lengths l_j; we suppose that at the 'loose ends' (if any), *Neumann condition is imposed*.

Using for $f \in \widetilde{H}^k(\Gamma) = \big\{ f : f_j \in H^k(0, l_j), j = 1, \dots, N \big\}$ the boundary values

$$F = (f_1(0), f_2(0), \dots, f_N(0))^\top \quad \text{and} \quad F' = (f_1'(0), f_2'(0), \dots, f_N'(0))^\top,$$

our operator is as before the (negative) Laplacian with the domain specified by the boundary conditions

$$(F_{j+1} - F_j) + i\left(F_j' + F_{j+1}'\right) = 0, \quad j = 1, \dots, N.$$

Remarks: Summing over j, we get $\sum_{j=1}^N F_j' = 0$. Moreover, if N is *even*, then summing with $(-1)^j$ leads to the relation $\sum_{j=1}^N F_j = 0$.

• Apart from the trivial case $N = 2$, the coupling *is not scale-invariant*; it has a nontrivial Robin component of dimension $2\lfloor \frac{N-1}{2} \rfloor$.

Spectral optimization: sesquilinear form

Proposition

The sesquilinear form of the described operator is for any $N \geq 2$ given by

$$\mathfrak{a}[f,g] = \sum_{j=1}^{N} \int_0^{l_j} f_j' \overline{g_j'} \,\mathrm{d}x + i \sum_{j=2}^{N} \sum_{k=1}^{j-1} (-1)^{j+k} \left(F_k \overline{G_j} - F_j \overline{G_k} \right)$$

with the domain

$$\mathrm{dom}\ \mathfrak{a} = \begin{cases} \widetilde{H}^1(\Gamma), & \textit{if } N \textit{ is odd}, \\ \left\{ f \in \widetilde{H}^1(\Gamma) : \sum_{j=1}^{N} (-1)^j F_j = 0 \right\}, & \textit{if } N \textit{ is even}, \end{cases}$$

being densely defined, symmetric, semi-bounded from below and closed.

Spectral optimization: sesquilinear form

Proposition

The sesquilinear form of the described operator is for any $N \geq 2$ given by

$$\mathfrak{a}[f,g] = \sum_{j=1}^{N} \int_0^{l_j} f_j' \overline{g_j'} \,\mathrm{d}x + i \sum_{j=2}^{N} \sum_{k=1}^{j-1} (-1)^{j+k} \left(F_k \overline{G_j} - F_j \overline{G_k} \right)$$

with the domain

$$\mathrm{dom}\ \mathfrak{a} = \begin{cases} \widetilde{H}^1(\Gamma), & \text{if } N \text{ is odd}, \\ \left\{ f \in \widetilde{H}^1(\Gamma) : \sum_{j=1}^{N} (-1)^j F_j = 0 \right\}, & \text{if } N \text{ is even}, \end{cases}$$

being densely defined, symmetric, semi-bounded from below and closed.

It is easy to see from here that the operator *is not positive* for any $N \geq 3$. It is enough to choose f_j constant on every edge, with $f_1 = 1$, $f_2 = i$, and $f_j = 0$ identically otherwise N is *odd*; and $f_1 = 1, f_2 = i, f_3 = -1, f_4 = -i$ and $f_j = 0$ identically for all further edges (if any) for N *even*.

Spectral optimization: sesquilinear form

Proposition

The sesquilinear form of the described operator is for any $N \geq 2$ given by

$$\mathfrak{a}[f,g] = \sum_{j=1}^{N} \int_0^{l_j} f_j' \overline{g_j'} \, \mathrm{d}x + i \sum_{j=2}^{N} \sum_{k=1}^{j-1} (-1)^{j+k} \left(F_k \overline{G_j} - F_j \overline{G_k} \right)$$

with the domain

$$\mathrm{dom}\ \mathfrak{a} = \begin{cases} \widetilde{H}^1(\Gamma), & \text{if } N \text{ is odd}, \\ \left\{ f \in \widetilde{H}^1(\Gamma) : \sum_{j=1}^{N} (-1)^j F_j = 0 \right\}, & \text{if } N \text{ is even}, \end{cases}$$

being densely defined, symmetric, semi-bounded from below and closed.

It is easy to see from here that the operator *is not positive* for any $N \geq 3$. It is enough to choose f_j constant on every edge, with $f_1 = 1$, $f_2 = i$, and $f_j = 0$ identically otherwise N is *odd*; and $f_1 = 1, f_2 = i, f_3 = -1, f_4 = -i$ and $f_j = 0$ identically for all further edges (if any) for N *even*.

However, we know that infinite star has $2\lfloor \frac{N-1}{2} \rfloor$ negative eigenvalues, and by *Neumann bracketing* any finite star has *at least as many*.

Spectral optimization: segment transplantation

Let Γ be a star graph with edge lengths $l_1, \dots, l_N$. We say that $\widetilde{\Gamma}$ is obtained from Γ by *transplanting a segment* of length $\ell \leq l_j$ from the edge e_j to the edge e_k if $\widetilde{\Gamma}$ is the star graph with edge lengths $\widetilde{l}_1, \dots, \widetilde{l}_N$, where $\widetilde{l}_j = l_j - \ell$, $\widetilde{l}_k = l_k + \ell$ and $\widetilde{l}_n = l_n$ whenever $n \neq j, k$

Spectral optimization: segment transplantation

Let Γ be a star graph with edge lengths $l_1, \ldots, l_N$. We say that $\widetilde{\Gamma}$ is obtained from Γ by *transplanting a segment* of length $\ell \leq l_j$ from the edge e_j to the edge e_k if $\widetilde{\Gamma}$ is the star graph with edge lengths $\widetilde{l_1}, \ldots, \widetilde{l_N}$, where $\widetilde{l_j} = l_j - \ell$, $\widetilde{l_k} = l_k + \ell$ and $\widetilde{l_n} = l_n$ whenever $n \neq j, k$ (if $\ell = l_j$, we have $\widetilde{l_j} = 0$ and $\widetilde{\Gamma}$ is a star graph of $N - 1$ edges).

Spectral optimization: segment transplantation

Let Γ be a star graph with edge lengths $l_1, \ldots, l_N$. We say that $\widetilde{\Gamma}$ is obtained from Γ by *transplanting a segment* of length $\ell \leq l_j$ from the edge e_j to the edge e_k if $\widetilde{\Gamma}$ is the star graph with edge lengths $\widetilde{l}_1, \ldots, \widetilde{l}_N$, where $\widetilde{l}_j = l_j - \ell$, $\widetilde{l}_k = l_k + \ell$ and $\widetilde{l}_n = l_n$ whenever $n \neq j, k$ (if $\ell = l_j$, we have $\widetilde{l}_j = 0$ and $\widetilde{\Gamma}$ is a star graph of $N - 1$ edges).

Proposition

Let Γ be a star graph with $N \geq 3$ edges and $\widetilde{\Gamma}$ is obtained from Γ by transplanting a segment of length $\ell < l_j$ from e_j to e_k. Then

$$\lambda_1(\widetilde{\Gamma}) < \lambda_1(\Gamma)$$

holds if $l_j \leq l_k$. The same holds true if $\ell = l_j$ and N is even.

Spectral optimization: segment transplantation

Let Γ be a star graph with edge lengths $l_1, \ldots, l_N$. We say that $\widetilde{\Gamma}$ is obtained from Γ by *transplanting a segment* of length $\ell \leq l_j$ from the edge e_j to the edge e_k if $\widetilde{\Gamma}$ is the star graph with edge lengths $\widetilde{l}_1, \ldots, \widetilde{l}_N$, where $\widetilde{l}_j = l_j - \ell$, $\widetilde{l}_k = l_k + \ell$ and $\widetilde{l}_n = l_n$ whenever $n \neq j, k$ (if $\ell = l_j$, we have $\widetilde{l}_j = 0$ and $\widetilde{\Gamma}$ is a star graph of $N-1$ edges).

Proposition

Let Γ be a star graph with $N \geq 3$ edges and $\widetilde{\Gamma}$ is obtained from Γ by transplanting a segment of length $\ell < l_j$ from e_j to e_k. Then

$$\lambda_1(\widetilde{\Gamma}) < \lambda_1(\Gamma)$$

holds if $l_j \leq l_k$. The same holds true if $\ell = l_j$ and N is even.

Proof sketch: We use Ansatz $\psi_j(x) = \alpha_j \cosh(\kappa(l_j - x))$ with $\lambda_1(\Gamma) = -\kappa^2$ for the ground state eigenfunction. The vertex conditions require

$$A_j \alpha_j + B_{j+1} \alpha_{j+1} = 0, \quad j = 1, \ldots, N,$$

where $A_j = \cosh(\kappa l_j) + i\kappa \sinh(\kappa l_j)$ and $B_j = -\cosh(\kappa l_j) + i\kappa \sinh(\kappa l_j)$.

Proof sketch

This means that $|A_j|^2 = |B_j|^2 = \cosh^2(\kappa l_j) + \kappa^2 \sinh^2(\kappa l_j)$ so that $|A_j|$ and $|B_j|$ are *strictly increasing* as functions of the edge length l_j.

Proof sketch

This means that $|A_j|^2 = |B_j|^2 = \cosh^2(\kappa l_j) + \kappa^2 \sinh^2(\kappa l_j)$ so that $|A_j|$ and $|B_j|$ are *strictly increasing* as functions of the edge length l_j.

Without loss of generality consider transplantation from e_1 to e_2 assuming that $l_1 \leq l_2$ and $\ell < l_1$. Then we choose on $\widetilde{\Gamma}$ a trial function setting

$$\widetilde{\psi}_1(x) = \psi_1(x), \quad x \in [0, \widetilde{l}_1],$$
$$\widetilde{\psi}_2(x) = \begin{cases} \psi_2(x), & x \in [0, l_2], \\ \frac{\alpha_2}{\alpha_1 \cosh(\kappa\ell)} \psi_1(x - l_2 + \widetilde{l}_1), & x \in [l_2, \widetilde{l}_2], \end{cases},$$

together with $\widetilde{\psi}_j = \psi_j$ for $j = 3, \ldots, N$, that is, we transplant a *scaled* piece of the eigenfunction from e_1 to e_2.

Proof sketch

This means that $|A_j|^2 = |B_j|^2 = \cosh^2(\kappa l_j) + \kappa^2 \sinh^2(\kappa l_j)$ so that $|A_j|$ and $|B_j|$ are *strictly increasing* as functions of the edge length l_j.

Without loss of generality consider transplantation from e_1 to e_2 assuming that $l_1 \leq l_2$ and $\ell < l_1$. Then we choose on $\widetilde{\Gamma}$ a trial function setting

$$\widetilde{\psi}_1(x) = \psi_1(x), \quad x \in [0, \widetilde{l}_1],$$

$$\widetilde{\psi}_2(x) = \begin{cases} \psi_2(x), & x \in [0, l_2], \\ \frac{\alpha_2}{\alpha_1 \cosh(\kappa\ell)} \psi_1(x - l_2 + \widetilde{l}_1), & x \in [l_2, \widetilde{l}_2], \end{cases},$$

together with $\widetilde{\psi}_j = \psi_j$ for $j = 3, \dots, N$, that is, we transplant a *scaled* piece of the eigenfunction from e_1 to e_2.

By a direct evaluation of the quadratic form, we then find

$$\widetilde{\mathfrak{a}}[\widetilde{\psi}] \leq \mathfrak{a}[\psi] = \lambda_1(\Gamma) \|\psi\|^2_{L^2(\Gamma)} \quad \text{and} \quad \|\psi\|^2 \geq \|\widetilde{\psi}\|^2_{L^2(\widetilde{\Gamma})}$$

giving the sought inequality $\widetilde{\mathfrak{a}}[\widetilde{\psi}] \leq \lambda_1(\Gamma) \|\widetilde{\psi}\|^2_{L^2(\widetilde{\Gamma})}$; recall that $\lambda_1(\Gamma) < 0$.

Proof sketch

This means that $|A_j|^2 = |B_j|^2 = \cosh^2(\kappa l_j) + \kappa^2 \sinh^2(\kappa l_j)$ so that $|A_j|$ and $|B_j|$ are *strictly increasing* as functions of the edge length l_j.

Without loss of generality consider transplantation from e_1 to e_2 assuming that $l_1 \leq l_2$ and $\ell < l_1$. Then we choose on $\widetilde{\Gamma}$ a trial function setting

$$\widetilde{\psi}_1(x) = \psi_1(x), \quad x \in [0, \widetilde{l}_1],$$

$$\widetilde{\psi}_2(x) = \begin{cases} \psi_2(x), & x \in [0, l_2], \\ \frac{\alpha_2}{\alpha_1 \cosh(\kappa\ell)} \psi_1(x - l_2 + \widetilde{l}_1), & x \in [l_2, \widetilde{l}_2], \end{cases},$$

together with $\widetilde{\psi}_j = \psi_j$ for $j = 3, \ldots, N$, that is, we transplant a *scaled* piece of the eigenfunction from e_1 to e_2.

By a direct evaluation of the quadratic form, we then find

$$\widetilde{\mathfrak{a}}[\widetilde{\psi}] \leq \mathfrak{a}[\psi] = \lambda_1(\Gamma) \|\psi\|^2_{L^2(\Gamma)} \quad \text{and} \quad \|\psi\|^2 \geq \|\widetilde{\psi}\|^2_{L^2(\widetilde{\Gamma})}$$

giving the sought inequality $\widetilde{\mathfrak{a}}[\widetilde{\psi}] \leq \lambda_1(\Gamma) \|\widetilde{\psi}\|^2_{L^2(\widetilde{\Gamma})}$; recall that $\lambda_1(\Gamma) < 0$.

The case $\ell = l_1$ is treated similarly, taking the domains into account.

What can transplantations achieve

By successive transplantations, we can eventually reach equilateral star.

Corollary

Assume that Γ is an arbitrary metric star graph with N edges and Γ^* is the equilateral star graph with N edges and the same total length as Γ. Then

$$\lambda_1(\Gamma) \leq \lambda_1(\Gamma^*)$$

holds. The inequality is saturated if and only if Γ is equilateral.

What can transplantations achieve

By successive transplantations, we can eventually reach equilateral star.

Corollary

Assume that Γ is an arbitrary metric star graph with N edges and Γ^* is the equilateral star graph with N edges and the same total length as Γ. Then

$$\lambda_1(\Gamma) \leq \lambda_1(\Gamma^*)$$

holds. The inequality is saturated if and only if Γ is equilateral.

In a similar way, we can compare equilateral stars with different edge numbers; we have to distinguish cases of *odd* and *even* N.

What can transplantations achieve

By successive transplantations, we can eventually reach equilateral star.

Corollary

Assume that Γ is an arbitrary metric star graph with N edges and Γ^* is the equilateral star graph with N edges and the same total length as Γ. Then

$$\lambda_1(\Gamma) \le \lambda_1(\Gamma^*)$$

holds. The inequality is saturated if and only if Γ is equilateral.

In a similar way, we can compare equilateral stars with different edge numbers; we have to distinguish cases of *odd* and *even* N.

Proposition

Denote by Γ_n^* the equilateral star graph with n edges and a fixed total length L. For any $N \ge 3$ the following inequalities hold:

1. $\lambda_1(\Gamma_{N+2}^*) < \lambda_1(\Gamma_N^*)$;

What can transplantations achieve

By successive transplantations, we can eventually reach equilateral star.

Corollary

Assume that Γ *is an arbitrary metric star graph with* N *edges and* Γ^* *is the* *equilateral* *star graph with* N *edges and the same total length as* Γ. *Then*

$$\lambda_1(\Gamma) \le \lambda_1(\Gamma^*)$$

holds. The inequality is saturated *if and only if* Γ *is equilateral.*

In a similar way, we can compare equilateral stars with different edge numbers; we have to distinguish cases of *odd* and *even* N.

Proposition

Denote by Γ_n^* *the equilateral star graph with* n *edges and a* *fixed total length* L. *For any* $N \ge 3$ *the following inequalities hold:*

1. $\lambda_1(\Gamma_{N+2}^*) < \lambda_1(\Gamma_N^*)$;
2. $\lambda_1(\Gamma_N^*) < \lambda_1(\Gamma_{N+1}^*)$ *if* N *is odd;*

What can transplantations achieve

By successive transplantations, we can eventually reach equilateral star.

Corollary

Assume that Γ is an arbitrary metric star graph with N edges and Γ^* is the equilateral star graph with N edges and the same total length as Γ. Then

$$\lambda_1(\Gamma) \leq \lambda_1(\Gamma^*)$$

holds. The inequality is saturated if and only if Γ is equilateral.

In a similar way, we can compare equilateral stars with different edge numbers; we have to distinguish cases of *odd* and *even* N.

Proposition

Denote by Γ_n^* the equilateral star graph with n edges and a fixed total length L. For any $N \geq 3$ the following inequalities hold:

1. $\lambda_1(\Gamma_{N+2}^*) < \lambda_1(\Gamma_N^*)$;
2. $\lambda_1(\Gamma_N^*) < \lambda_1(\Gamma_{N+1}^*)$ *if N is odd; and*
3. $\lambda_1(\Gamma_{N+1}^*) < \lambda_1(\Gamma_N^*)$ *if N is even.*

What can transplantations achieve

Using the last two claims, one can obtain easily an optimization result for the star graphs ground state eigenvalue:

Theorem

Let $L > 0$ and let Γ be a metric star graph with $N \geq 3$ edges and total length L. If we denote by Γ_3^* and Γ_4^* the equilateral star graphs with three and four edges, respectively, of total length L, then

$$\lambda_1(\Gamma) \leq \begin{cases} \lambda_1(\Gamma_3^*), & \text{if } N \text{ is odd,} \\ \lambda_1(\Gamma_4^*), & \text{if } N \text{ is even,} \end{cases}$$

holds, with the inequalities being saturated if and only if $\Gamma = \Gamma_3^*$ (if N is odd) or $\Gamma = \Gamma_4^*$ (if N is even).

Surgeries beyond transplantations

Next we pass to more complicated surgical operations on star graphs in which the volume can be *added* or *removed*.

Proposition

Let Γ be a star graph of $N \geq 2$ edges and $\widetilde{\Gamma}$ a star obtained by adding one edge rooted in the common vertex. Then we have $\lambda_k(\widetilde{\Gamma}) \leq \lambda_k(\Gamma)$

1. *for all $k \in \mathbb{N}$ if N is even;*

Surgeries beyond transplantations

Next we pass to more complicated surgical operations on star graphs in which the volume can be *added* or *removed*.

Proposition

Let Γ be a star graph of $N \geq 2$ edges and $\widetilde{\Gamma}$ a star obtained by adding one edge rooted in the common vertex. Then we have $\lambda_k(\widetilde{\Gamma}) \leq \lambda_k(\Gamma)$

1. *for all $k \in \mathbb{N}$ if N is even; and*
2. *for all $k \in \mathbb{N}$ such that $\lambda_k(\Gamma) \geq 0$ if N is odd.*

Surgeries beyond transplantations

Next we pass to more complicated surgical operations on star graphs in which the volume can be *added* or *removed*.

Proposition

Let Γ be a star graph of $N \geq 2$ edges and $\widetilde{\Gamma}$ a star obtained by adding one edge rooted in the common vertex. Then we have $\lambda_k(\widetilde{\Gamma}) \leq \lambda_k(\Gamma)$

1. *for all $k \in \mathbb{N}$ if N is even; and*
2. *for all $k \in \mathbb{N}$ such that $\lambda_k(\Gamma) \geq 0$ if N is odd.*

The proof uses min-max principle again: in the first case we construct trial functions *extending any $f \in \mathrm{dom}\, \mathfrak{a}$ by zero* on the added edge

Surgeries beyond transplantations

Next we pass to more complicated surgical operations on star graphs in which the volume can be *added* or *removed*.

Proposition

Let Γ be a star graph of $N \geq 2$ edges and $\widetilde{\Gamma}$ a star obtained by adding one edge rooted in the common vertex. Then we have $\lambda_k(\widetilde{\Gamma}) \leq \lambda_k(\Gamma)$

1. *for all $k \in \mathbb{N}$ if N is even; and*
2. *for all $k \in \mathbb{N}$ such that $\lambda_k(\Gamma) \geq 0$ if N is odd.*

The proof uses min-max principle again: in the first case we construct trial functions *extending any $f \in \mathrm{dom}\, \mathfrak{a}$ by zero* on the added edge, in the second we extend it by *constant function* equal to $\sum_{j=1}^{N} (-1)^{j+1} F_j$ on the added edge; in this case we need $\lambda_k(\Gamma) \geq 0$ to get the needed inequality between the quadratic forms

Surgeries beyond transplantations

Next we pass to more complicated surgical operations on star graphs in which the volume can be *added* or *removed*.

Proposition

Let Γ be a star graph of $N \geq 2$ edges and $\widetilde{\Gamma}$ a star obtained by adding one edge rooted in the common vertex. Then we have $\lambda_k(\widetilde{\Gamma}) \leq \lambda_k(\Gamma)$

1. *for all $k \in \mathbb{N}$ if N is even; and*
2. *for all $k \in \mathbb{N}$ such that $\lambda_k(\Gamma) \geq 0$ if N is odd.*

The proof uses min-max principle again: in the first case we construct trial functions *extending any $f \in \mathrm{dom}\, \mathfrak{a}$ by zero* on the added edge, in the second we extend it by *constant function* equal to $\sum_{j=1}^{N} (-1)^{j+1} F_j$ on the added edge; in this case we need $\lambda_k(\Gamma) \geq 0$ to get the needed inequality between the quadratic forms. In the analogous way we get

Proposition

Let Γ be a star graph with an even number of edges and $\widetilde{\Gamma}$ be obtained by attaching any even number of edges. Then $\lambda_k(\widetilde{\Gamma}) \leq \lambda_k(\Gamma)$ for all $k \in \mathbb{N}$.

Surgeries beyond transplantations

Removing in successive steps pairs of edges until we reach the case $N = 2$ which is nothing but Neumann Laplacian on an interval, we get

Corollary

Let Γ be a star graph with an even number $N \geq 2$ of edges. Then

$$\lambda_k(\Gamma) \leq \frac{(k-1)^2\pi^2}{\mathrm{diam}(\Gamma)^2} \leq \frac{(k-1)^2\pi^2 N^2}{4L(\Gamma)^2} = \frac{(k-1)^2\pi^2}{4A(\Gamma)^2}$$

holds for all $k \in \mathbb{N}$, where $L(\Gamma)$ denotes the total length of Γ, $A(\Gamma)$ the arithmetic mean of the edge lengths, and $\mathrm{diam}(\Gamma)$ metric diameter of Γ.

Surgeries beyond transplantations

Removing in successive steps pairs of edges until we reach the case $N = 2$ which is nothing but Neumann Laplacian on an interval, we get

Corollary

Let Γ be a star graph with an even number $N \geq 2$ of edges. Then

$$\lambda_k(\Gamma) \leq \frac{(k-1)^2\pi^2}{\mathrm{diam}(\Gamma)^2} \leq \frac{(k-1)^2\pi^2 N^2}{4L(\Gamma)^2} = \frac{(k-1)^2\pi^2}{4A(\Gamma)^2}$$

holds for all $k \in \mathbb{N}$, where $L(\Gamma)$ denotes the total length of Γ, $A(\Gamma)$ the arithmetic mean of the edge lengths, and $\mathrm{diam}(\Gamma)$ metric diameter of Γ.

Note that the *bound is trivial for $k = 1$* as it only yields $\lambda_1(\Gamma) \leq 0$.

Surgeries beyond transplantations

Removing in successive steps pairs of edges until we reach the case $N = 2$ which is nothing but Neumann Laplacian on an interval, we get

Corollary

Let Γ be a star graph with an even number $N \geq 2$ of edges. Then

$$\lambda_k(\Gamma) \leq \frac{(k-1)^2\pi^2}{\mathrm{diam}(\Gamma)^2} \leq \frac{(k-1)^2\pi^2 N^2}{4L(\Gamma)^2} = \frac{(k-1)^2\pi^2}{4A(\Gamma)^2}$$

holds for all $k \in \mathbb{N}$, where $L(\Gamma)$ denotes the total length of Γ, $A(\Gamma)$ the arithmetic mean of the edge lengths, and $\mathrm{diam}(\Gamma)$ metric diameter of Γ.

Note that the *bound is trivial for $k = 1$* as it only yields $\lambda_1(\Gamma) \leq 0$.

It is also easy to see what an enlargement of an edge length does:

Proposition

Let $\widetilde{\Gamma}$ be obtained from Γ by enlarging the length of an edge, then

1. *If $\lambda_k(\widetilde{\Gamma}) \leq 0$, then $\lambda_k(\Gamma) \leq \lambda_k(\widetilde{\Gamma})$, in particular, $\lambda_1(\Gamma) \leq \lambda_1(\widetilde{\Gamma})$.*
2. *If $\lambda_k(\Gamma) \geq 0$, then $\lambda_k(\widetilde{\Gamma}) \leq \lambda_k(\Gamma)$.*

A digression: Dirichlet endpoints

The first part of the last claim changes if we consider star graphs with Dirichlet endpoints, i.e. the operator associated with the form

$$\mathfrak{a}_{\mathrm{D}}[f,g] = \sum_{j=1}^{N} \int_0^{l_j} f_j' \overline{g_j'}\, \mathrm{d}x + i \sum_{j=2}^{N} \sum_{k=1}^{j-1} (-1)^{j+k} \left(F_k \overline{G_j} - F_j \overline{G_k} \right)$$

which differs from the previous one by its domain,

$$\mathrm{dom}\ \mathfrak{a}_{\mathrm{D}} = \begin{cases} \left\{ f \in \widetilde{H}^1(\Gamma) :\, f(v_j) = 0,\, j = 1,\dots,N \right\} & \text{for } N \text{ odd}, \\ \left\{ f \in \widetilde{H}^1(\Gamma) :\, \sum_{j=1}^{N} (-1)^j F_j = 0,\, f(v_j) = 0,\, j = 1,\dots,N \right\} & \text{for } N \text{ even}. \end{cases}$$

A digression: Dirichlet endpoints

The first part of the last claim changes if we consider star graphs with Dirichlet endpoints, i.e. the operator associated with the form

$$\mathfrak{a}_{\mathrm{D}}[f,g] = \sum_{j=1}^{N} \int_0^{l_j} f_j' \overline{g_j'}\, \mathrm{d}x + i \sum_{j=2}^{N} \sum_{k=1}^{j-1} (-1)^{j+k} \left(F_k \overline{G_j} - F_j \overline{G_k} \right)$$

which differs from the previous one by its domain,

$$\mathrm{dom}\ \mathfrak{a}_{\mathrm{D}} = \begin{cases} \left\{ f \in \widetilde{H}^1(\Gamma) : f(v_j) = 0,\, j = 1, \dots, N \right\} & \text{for } N \text{ odd}, \\ \left\{ f \in \widetilde{H}^1(\Gamma) : \sum_{j=1}^{N} (-1)^j F_j = 0,\, f(v_j) = 0,\, j = 1, \dots, N \right\} & \text{for } N \text{ even}. \end{cases}$$

Proposition

In this case, if $\widetilde{\Gamma}$ is obtained from Γ by enlarging the length of an edge, the eigenvalues satisfy the inequality

$$\lambda_k(\widetilde{\Gamma}) \le \lambda_k(\Gamma) \quad \textit{for all } k \in \mathbb{N}.$$

Beyond star graphs

Let us turn now to a more general situation and suppose that Γ is a *compact, finite metric graph*; at vertices of degree ≥ 3 the indicated matching conditions hold, and *Neumann* ones at the 'loose' endpoints.

Beyond star graphs

Let us turn now to a more general situation and suppose that Γ is a *compact, finite metric graph*; at vertices of degree ≥ 3 the indicated matching conditions hold, and *Neumann* ones at the 'loose' endpoints.

The spectrum is given by *secular equation* combining the matching condition with *Dirichlet-to-Neumann matrices* at the edges. We set

$$\begin{pmatrix} A_m \\ B_m \end{pmatrix} := \begin{pmatrix} 1 & \mp 1 & 0 & \cdots & \cdots & 0 \\ 0 & \ddots & \ddots & \ddots & & \vdots \\ \vdots & \ddots & \ddots & \ddots & \ddots & \vdots \\ \vdots & & \ddots & \ddots & \ddots & 0 \\ 0 & \cdots & \cdots & 0 & \ddots & \mp 1 \\ \mp 1 & 0 & \cdots & \cdots & 0 & 1 \end{pmatrix} \in \mathbb{C}^{\deg(v_m)\times\deg(v_m)}$$

in case $\deg(v_m) \geq 2$, and $\binom{A_m}{B_m} := \binom{0}{1}$ in case $\deg(v_m) = 1$, and put

$$\mathcal{A} := \operatorname{diag}(A_1, \dots, A_n) \quad \text{and} \quad \mathcal{B} := \operatorname{diag}(B_1, \dots, B_n).$$

Beyond star graphs

Let us turn now to a more general situation and suppose that Γ is a *compact, finite metric graph*; at vertices of degree ≥ 3 the indicated matching conditions hold, and *Neumann* ones at the 'loose' endpoints.

The spectrum is given by *secular equation* combining the matching condition with *Dirichlet-to-Neumann matrices* at the edges. We set

$$\binom{A_m}{B_m} := \begin{pmatrix} 1 & \mp 1 & 0 & \cdots & \cdots & 0 \\ 0 & \ddots & \ddots & \ddots & & \vdots \\ \vdots & \ddots & \ddots & \ddots & \ddots & \vdots \\ \vdots & & \ddots & \ddots & \ddots & 0 \\ 0 & \cdots & \cdots & 0 & \ddots & \mp 1 \\ \mp 1 & 0 & \cdots & \cdots & 0 & 1 \end{pmatrix} \in \mathbb{C}^{\deg(v_m)\times\deg(v_m)}$$

in case $\deg(v_m) \geq 2$, and $\binom{A_m}{B_m} := \binom{0}{1}$ in case $\deg(v_m) = 1$, and put

$$\mathcal{A} := \mathrm{diag}(A_1, \dots, A_n) \quad \text{and} \quad \mathcal{B} := \mathrm{diag}(B_1, \dots, B_n).$$

The D-to-N matrix is $M(\lambda)$ is block-diagonal with the elements $M_l(\lambda) = \kappa \begin{pmatrix} -\coth(\kappa l) & \frac{1}{\sinh(\kappa l)} \\ \frac{1}{\sinh(\kappa l)} & -\coth(\kappa l) \end{pmatrix}$ for $\lambda = -\kappa^2$; for $\lambda > 0$ we use the trigonometric analogue staying away of Dirichlet eigenvalues.

The secular equation

With this notation, we can state the sought equation: for a given λ, a function $f \in \widetilde{H}^2(\Gamma)$ solving $-f'' = \lambda f$ on each of the edges satisfies the vertex conditions if and only if

$$(\mathcal{A} + i\mathcal{B}M(\lambda)) \begin{pmatrix} F(v_1) \\ \vdots \\ F(v_n) \end{pmatrix} = 0,$$

The secular equation

With this notation, we can state the sought equation: for a given λ, a function $f \in \widetilde{H}^2(\Gamma)$ solving $-f'' = \lambda f$ on each of the edges satisfies the vertex conditions if and only if

$$(\mathcal{A} + i\mathcal{B}M(\lambda)) \begin{pmatrix} F(v_1) \\ \vdots \\ F(v_n) \end{pmatrix} = 0,$$

and consequently, λ is an eigenvalue of our operator if and only if

$$\det(\mathcal{A} + i\mathcal{B}M(\lambda)) = 0.$$

The secular equation

With this notation, we can state the sought equation: for a given λ, a function $f \in \widetilde{H}^2(\Gamma)$ solving $-f'' = \lambda f$ on each of the edges satisfies the vertex conditions if and only if

$$(\mathcal{A} + i\mathcal{B}M(\lambda)) \begin{pmatrix} F(v_1) \\ \vdots \\ F(v_n) \end{pmatrix} = 0,$$

and consequently, λ is an eigenvalue of our operator if and only if

$$\det(\mathcal{A} + i\mathcal{B}M(\lambda)) = 0.$$

Remark: The vertex conditions depend on a fixed choice of an order of the edge endpoints in vertex v, however, an inspection of the secular equation shows that the spectrum of the operator is independent of it.

Figure-8 graph

Example

Consider Γ with one vertex and two loops of lengths l_1 and l_2 meeting at it. Using the Ansatz $\psi_j(x) = \alpha_j \cosh(\kappa x) + \beta_j \sinh(\kappa x)$ for $x \in [0, l_j]$, we get from the secular equation the spectral condition

$$-16i\kappa(\kappa^2 - 1) \sinh \frac{\kappa l_1}{2} \sinh \frac{\kappa l_2}{2} \sinh \frac{\kappa(l_1 + l_2)}{2} = 0.$$

Figure-8 graph

Example

Consider Γ with one vertex and two loops of lengths l_1 and l_2 meeting at it. Using the Ansatz $\psi_j(x) = \alpha_j \cosh(\kappa x) + \beta_j \sinh(\kappa x)$ for $x \in [0, l_j]$, we get from the secular equation the spectral condition

$$-16i\kappa(\kappa^2 - 1)\sinh\frac{\kappa l_1}{2}\sinh\frac{\kappa l_2}{2}\sinh\frac{\kappa(l_1 + l_2)}{2} = 0.$$

Consequently, $\lambda_1(\Gamma) = -1$ is the only negative eigenvalue, independently of l_1 and l_2 and the enumeration of the edges' endpoints.

Figure-8 graph

Example

Consider Γ with one vertex and two loops of lengths l_1 and l_2 meeting at it. Using the Ansatz $\psi_j(x) = \alpha_j \cosh(\kappa x) + \beta_j \sinh(\kappa x)$ for $x \in [0, l_j]$, we get from the secular equation the spectral condition

$$-16i\kappa(\kappa^2 - 1) \sinh \frac{\kappa l_1}{2} \sinh \frac{\kappa l_2}{2} \sinh \frac{\kappa(l_1 + l_2)}{2} = 0.$$

Consequently, $\lambda_1(\Gamma) = -1$ is the only negative eigenvalue, independently of l_1 and l_2 and the enumeration of the edges' endpoints.

For positive energies $\lambda = k^2$ with $k > 0$, the spectral condition reads

$$\sin(kl_1) + \sin(kl_2) - \sin(k(l_1 + l_2)) = 0.$$

Figure-8 graph

Example

Consider Γ with one vertex and two loops of lengths l_1 and l_2 meeting at it. Using the Ansatz $\psi_j(x) = \alpha_j \cosh(\kappa x) + \beta_j \sinh(\kappa x)$ for $x \in [0, l_j]$, we get from the secular equation the spectral condition

$$-16i\kappa(\kappa^2 - 1)\sinh\frac{\kappa l_1}{2}\sinh\frac{\kappa l_2}{2}\sinh\frac{\kappa(l_1 + l_2)}{2} = 0.$$

Consequently, $\lambda_1(\Gamma) = -1$ is the only negative eigenvalue, independently of l_1 and l_2 and the enumeration of the edges' endpoints.

For positive energies $\lambda = k^2$ with $k > 0$, the spectral condition reads

$$\sin(kl_1) + \sin(kl_2) - \sin(k(l_1 + l_2)) = 0.$$

Obviously, this positive spectrum *scales* with simultaneous change of the loop lengths. For $l_1 + l_2 = 1$, the condition is clearly satisfied if $k = 2n\pi$ for some $n \in \mathbb{N}$

Figure-8 graph

Example

Consider Γ with one vertex and two loops of lengths l_1 and l_2 meeting at it. Using the Ansatz $\psi_j(x) = \alpha_j \cosh(\kappa x) + \beta_j \sinh(\kappa x)$ for $x \in [0, l_j]$, we get from the secular equation the spectral condition

$$-16i\kappa(\kappa^2 - 1) \sinh \frac{\kappa l_1}{2} \sinh \frac{\kappa l_2}{2} \sinh \frac{\kappa(l_1 + l_2)}{2} = 0.$$

Consequently, $\lambda_1(\Gamma) = -1$ is the only negative eigenvalue, independently of l_1 and l_2 and the enumeration of the edges' endpoints.

For positive energies $\lambda = k^2$ with $k > 0$, the spectral condition reads

$$\sin(kl_1) + \sin(kl_2) - \sin(k(l_1 + l_2)) = 0.$$

Obviously, this positive spectrum *scales* with simultaneous change of the loop lengths. For $l_1 + l_2 = 1$, the condition is clearly satisfied if $k = 2n\pi$ for some $n \in \mathbb{N}$. In general, there may by other positive eigenvalues. In the equilateral case, however, the condition simplifies $\sin(k) = 2\sin(\frac{k}{2})$, and the positive eigenvalues are given just by the numbers $(2n\pi)^2$ with multiplicity *one if n is odd* and *three if n is even*.

Toolbox revisited

To prove our first main result with combine two techniques:

Toolbox revisited

To prove our first main result with combine two techniques:

The first basic tool is the *sesquilinear form* associated with Laplacian on Γ: we get it simply as the *sum of the 'elementary' forms* described above. Specifically, we sum the integral parts over the edges, and the boundary-values parts over the vertices.

Toolbox revisited

To prove our first main result with combine two techniques:

The first basic tool is the *sesquilinear form* associated with Laplacian on Γ: we get it simply as the *sum of the 'elementary' forms* described above. Specifically, we sum the integral parts over the edges, and the boundary-values parts over the vertices.

Secondly, we will employ additional *surgical operations:* Consider vertices $v_1, v_2 \in \mathcal{V}(\Gamma)$; we say that $\widetilde{\Gamma}$ is obtained from Γ by *merging* v_1 and v_2, or equivalently, that Γ *is be obtained from* $\widetilde{\Gamma}$ *by splitting a vertex* $\hat{v}$ if $\widetilde{\Gamma}$ has *the same set of edges* as Γ, $\mathcal{E}(\widetilde{\Gamma}) = \mathcal{E}(\Gamma)$, its vertex set equals

$$\mathcal{V}(\widetilde{\Gamma}) = (\mathcal{V}(\Gamma) \setminus \{v_1, v_2\}) \cup \{\hat{v}\},$$

and the edges of the original graph Γ which met in v_1, v_2, meet in $\widetilde{\Gamma}$ instead in the new vertex $\hat{v}$.

Technique to be used

Let us now look what a needle and scalpel application to the graph causes. As before we have to distinguish cases of different parities:

Technique to be used

Let us now look what a needle and scalpel application to the graph causes. As before we have to distinguish cases of different parities:

Proposition

Let $\widetilde{\Gamma}$ be obtained from Γ by merging vertices $v_1, v_2 \in \mathcal{V}$. Then the following inequalities hold:

1. *If $\deg(v_1) + \deg(v_2)$ is odd, i.e. v_1 and v_2 have opposite parity, then*

$$\lambda_k(\widetilde{\Gamma}) \leq \lambda_k(\Gamma) \quad \text{for all} \quad k \in \mathbb{N}.$$

Technique to be used

Let us now look what a needle and scalpel application to the graph causes. As before we have to distinguish cases of different parities:

Proposition

Let $\widetilde{\Gamma}$ be obtained from Γ by merging vertices $v_1, v_2 \in \mathcal{V}$. Then the following inequalities hold:

1. *If $\deg(v_1) + \deg(v_2)$ is odd, i.e. v_1 and v_2 have opposite parity, then*

$$\lambda_k(\widetilde{\Gamma}) \leq \lambda_k(\Gamma) \quad \textit{for all} \quad k \in \mathbb{N}.$$

2. *If both $\deg(v_1)$ and $\deg(v_2)$ are even, then the same is true.*

Technique to be used

Let us now look what a needle and scalpel application to the graph causes. As before we have to distinguish cases of different parities:

Proposition

Let $\widetilde{\Gamma}$ be obtained from Γ by merging vertices $v_1, v_2 \in \mathcal{V}$. Then the following inequalities hold:

1. *If* $\deg(v_1) + \deg(v_2)$ *is odd, i.e.* v_1 *and* v_2 *have opposite parity, then*
$$\lambda_k(\widetilde{\Gamma}) \leq \lambda_k(\Gamma) \quad \textit{for all} \quad k \in \mathbb{N}.$$
2. *If both* $\deg(v_1)$ *and* $\deg(v_2)$ *are even, then the same is true.*
3. *If both* $\deg(v_1)$ *and* $\deg(v_2)$ *are odd, then we have*
$$\lambda_k(\Gamma) \leq \lambda_k(\widetilde{\Gamma}) \quad \textit{for all} \quad k \in \mathbb{N}.$$

Technique to be used

Let us now look what a needle and scalpel application to the graph causes. As before we have to distinguish cases of different parities:

Proposition

Let $\widetilde{\Gamma}$ be obtained from Γ by merging vertices $v_1, v_2 \in \mathcal{V}$. Then the following inequalities hold:

1. *If $\deg(v_1) + \deg(v_2)$ is odd, i.e. v_1 and v_2 have opposite parity, then*
$$\lambda_k(\widetilde{\Gamma}) \leq \lambda_k(\Gamma) \quad \text{for all} \quad k \in \mathbb{N}.$$
2. *If both $\deg(v_1)$ and $\deg(v_2)$ are even, then the same is true.*
3. *If both $\deg(v_1)$ and $\deg(v_2)$ are odd, then we have*
$$\lambda_k(\Gamma) \leq \lambda_k(\widetilde{\Gamma}) \quad \text{for all} \quad k \in \mathbb{N}.$$

Everything follows from comparisons of the corresponding quadratic forms.

First main result

Let us now apply this to a general graph Γ excluding the trivial cases.

First main result

Let us now apply this to a general graph Γ excluding the trivial cases.
First we merge all *odd-degree vertices* obtaining a graph with *all degrees even*, among them at least one of *degree four*.

First main result

Let us now apply this to a general graph Γ excluding the trivial cases. First we merge all *odd-degree vertices* obtaining a graph with *all degrees even*, among them at least one of *degree four*.

Next we keep *splitting the remaining even-degree vertices* in such a way that the *Eulerian cycles* remain preserved; in this way we finally arrive at a *figure-8 graph*. This yields:

First main result

Let us now apply this to a general graph Γ excluding the trivial cases. First we merge all *odd-degree vertices* obtaining a graph with *all degrees even*, among them at least one of *degree four*.

Next we keep *splitting the remaining even-degree vertices* in such a way that the *Eulerian cycles* remain preserved; in this way we finally arrive at a *figure-8 graph*. This yields:

Theorem

Let Γ be a finite, compact metric graph of the considered type, different from a path graph or a cycle graph. Then the inequalities

$$\lambda_1(\Gamma) \leq -1, \;\; \lambda_2(\Gamma) \leq 0 \;\; \textit{and} \;\; \lambda_{2k+1}(\Gamma) \leq \frac{4k^2\pi^2}{L(\Gamma)^2}, \;\; k = 1, 2, \dots,$$

hold. In particular, there exists at least one negative eigenvalue

First main result

Let us now apply this to a general graph Γ excluding the trivial cases. First we merge all *odd-degree vertices* obtaining a graph with *all degrees even*, among them at least one of *degree four*.

Next we keep *splitting the remaining even-degree vertices* in such a way that the *Eulerian cycles* remain preserved; in this way we finally arrive at a *figure-8 graph*. This yields:

Theorem

Let Γ be a finite, compact metric graph of the considered type, different from a path graph or a cycle graph. Then the inequalities

$$\lambda_1(\Gamma) \leq -1, \;\; \lambda_2(\Gamma) \leq 0 \;\; \textit{and} \;\; \lambda_{2k+1}(\Gamma) \leq \frac{4k^2\pi^2}{L(\Gamma)^2}, \;\; k = 1, 2, \dots,$$

hold. In particular, there exists at least one negative eigenvalue. Moreover, these estimates cannot be improved.

P.E., J. Rohleder: Optimization of quantum graph eigenvalues with preferred orientation vertex conditions, *Ann H. Poincaré* **27** (2026), 1971–2001.

The second example: quantum chaos

Since the pioneering work of Kottos and Smilansky,

T. Kottos, U. Smilansky: Quantum chaos on graphs, *Phys. Rev. Lett.* **79** (1997), 4794–4797.

we know that quantum graphs are provide a suitable environment to investigate *quantum chaos*

The second example: quantum chaos

Since the pioneering work of Kottos and Smilansky,

T. Kottos, U. Smilansky: Quantum chaos on graphs, *Phys. Rev. Lett.* **79** (1997), 4794–4797.

we know that quantum graphs are provide a suitable environment to investigate *quantum chaos*. Specifically, the established paradigm is that – in the absence of spin – the spectral statistics of ‘sufficiently connected’ graphs with incommensurate edges falls into one of two *universal random matrix classes:*

- *Gaussian Orthogonal Ensemble (GOE)* provided the system is *time reversal invariant*

The second example: quantum chaos

Since the pioneering work of Kottos and Smilansky,

T. Kottos, U. Smilansky: Quantum chaos on graphs, *Phys. Rev. Lett.* **79** (1997), 4794–4797.

we know that quantum graphs are provide a suitable environment to investigate *quantum chaos*. Specifically, the established paradigm is that – in the absence of spin – the spectral statistics of 'sufficiently connected' graphs with incommensurate edges falls into one of two *universal random matrix classes:*

- *Gaussian Orthogonal Ensemble (GOE)* provided the system is *time reversal invariant*
- *Gaussian Unitary Ensemble (GUE)* if the invariance is violated, typically by the presence of a *magnetic field*

The second example: quantum chaos

Since the pioneering work of Kottos and Smilansky,

T. Kottos, U. Smilansky: Quantum chaos on graphs, *Phys. Rev. Lett.* **79** (1997), 4794–4797.

we know that quantum graphs are provide a suitable environment to investigate *quantum chaos*. Specifically, the established paradigm is that – in the absence of spin – the spectral statistics of 'sufficiently connected' graphs with incommensurate edges falls into one of two *universal random matrix classes:*

- *Gaussian Orthogonal Ensemble (GOE)* provided the system is *time reversal invariant*
- *Gaussian Unitary Ensemble (GUE)* if the invariance is violated, typically by the presence of a *magnetic field*

Graphs with the R coupling in the vertices, our basic example,

$$(\psi_{j+1} - \psi_j) + i(\psi'_{j+1} + \psi'_j) = 0\,, \quad j \in \mathbb{Z} \pmod n,$$

allow us to *challenge this paradigm* using simple graphs

The quantities to be inspected

We denote by $\{k_n\}_{n=1}^{\infty}$ the square roots of the eigenvalues of a finite quantum graph and consider the *nearest-neighbour spacing distribution*,

$$P(x) = \lim_{N\to\infty} \frac{1}{N} \sum_{i=1}^{N} \delta(x - (k_{i+1} - k_i))$$

Finer properties are manifested in the *two-point correlation function*

$$R_2(x) = \lim_{N\to\infty} \frac{1}{N} \sum_{i=1}^{N} \sum_{j=1}^{N} \delta(x - (k_j - k_i))$$

and the Fourier transform of $R_2(x)$ called the *form factor*,

$$K(\tau) = \int_{-\infty}^{\infty} \mathrm{e}^{2\pi i x \tau} (R_2(x) - 1)\, \mathrm{d}x$$

The quantities to be inspected

We denote by $\{k_n\}_{n=1}^{\infty}$ the square roots of the eigenvalues of a finite quantum graph and consider the *nearest-neighbour spacing distribution*,

$$P(x) = \lim_{N\to\infty} \frac{1}{N} \sum_{i=1}^{N} \delta(x - (k_{i+1} - k_i))$$

Finer properties are manifested in the *two-point correlation function*

$$R_2(x) = \lim_{N\to\infty} \frac{1}{N} \sum_{i=1}^{N} \sum_{j=1}^{N} \delta(x - (k_j - k_i))$$

and the Fourier transform of $R_2(x)$ called the *form factor*,

$$K(\tau) = \int_{-\infty}^{\infty} \mathrm{e}^{2\pi i x\tau} (R_2(x) - 1)\, \mathrm{d}x$$

Note that in graphs the eigenvalue counting function satisfies, for *any* vertex conditions, the Weyl's law, $N(k) = \frac{L}{\pi} k + \mathcal{O}(1)$ as $k \to \infty$, where $L = \sum_j \ell_j$ is the total length, hence the needed *scale unfolding* is trivial.

J. Bolte, S. Endres: The trace formula for quantum graphs with general self adjoint boundary conditions, *Ann. Henri Poincaré*, **10** (2009), 189–223.

The incommensurate octahedron graph

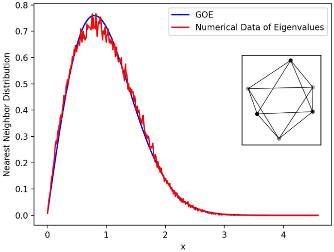

The incommensurate octahedron graph

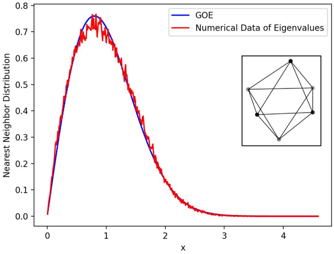

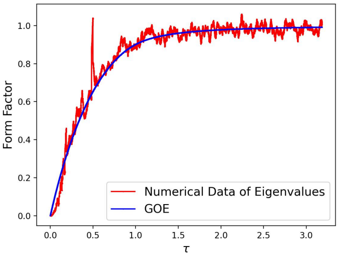

The incommensurate octahedron graph

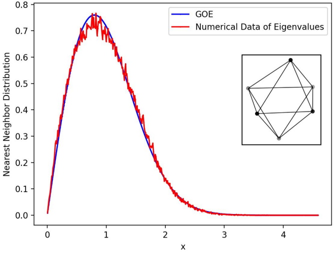

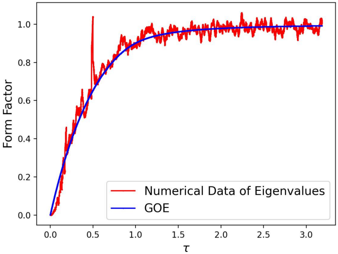

The first figure shows that eigenvalue spacing distribution fits nicely with the GOE and *not the GUE*, despite the fact the graph violates the time reversal symmetry.

The incommensurate octahedron graph

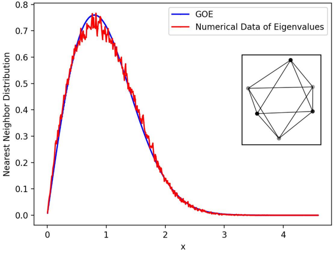

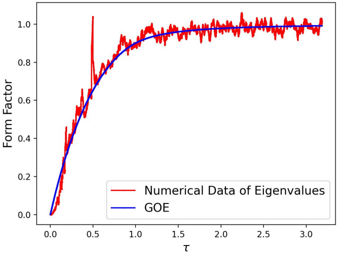

The first figure shows that eigenvalue spacing distribution fits nicely with the GOE and *not the GUE*, despite the fact the graph violates the time reversal symmetry.

The form factor also generally coincides with the GOE prediction, however, there is a *significant deviation*, namely the sharp peak at $\tau = \frac{1}{2}$.

R. Band, P.E., D. Goel, A. Strauss: Spectral statistics of preferred orientation quantum graphs, *J. Math. Phys.* **67** (2026), 013502

The incommensurate octahedron graph

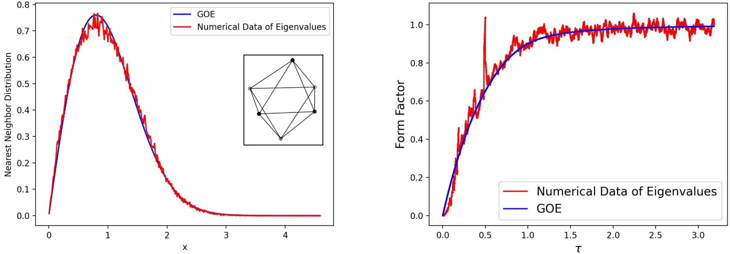

The first figure shows that eigenvalue spacing distribution fits nicely with the GOE and *not the GUE*, despite the fact the graph violates the time reversal symmetry.

The form factor also generally coincides with the GOE prediction, however, there is a *significant deviation*, namely the sharp peak at $\tau = \frac{1}{2}$.

R. Band, P.E., D. Goel, A. Strauss: Spectral statistics of preferred orientation quantum graphs, *J. Math. Phys.* **67** (2026), 013502

Before explaining these observations, note that the effect disappears if the edges are *asymptotically disconnected* at high energies.

Asymptotically disconnected edges

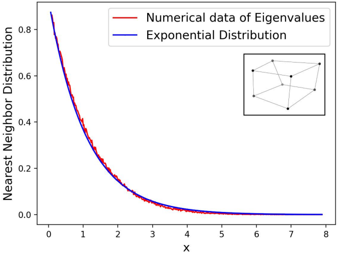

Asymptotically disconnected edges

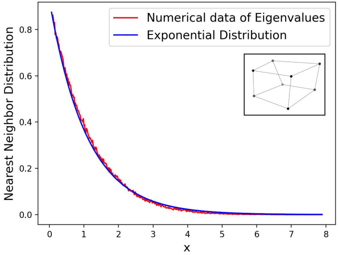

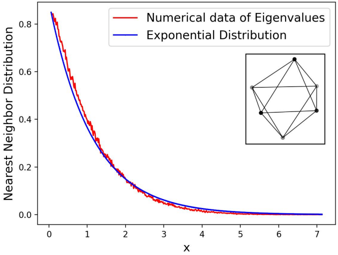

Asymptotically disconnected edges

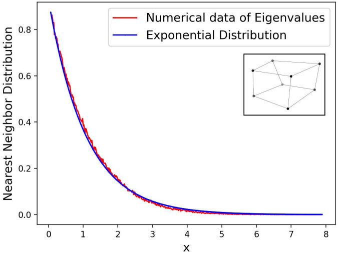

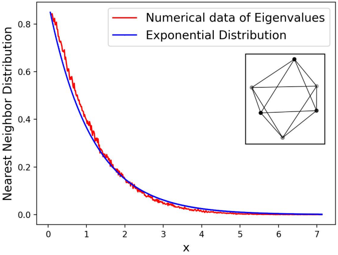

The first figure shows the (incommensurate) *cube* graph with the R coupling; as we know, in this situation vertices of *degree three* are asymptotically decoupled at high energies.

Asymptotically disconnected edges

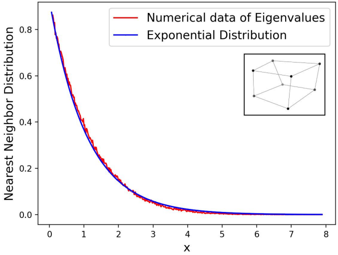

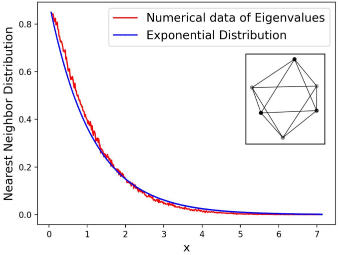

The first figure shows the (incommensurate) *cube* graph with the R coupling; as we know, in this situation vertices of *degree three* are asymptotically decoupled at high energies.

In the other we have an octahedron but the coupling matrix is changed to $U = \mathrm{e}^{i\mu}R$ with $\mu = 0.01$; as a result -1 is not an eigenvalue of U.

Asymptotically disconnected edges

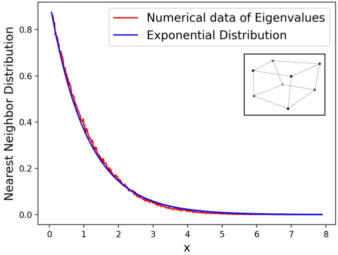

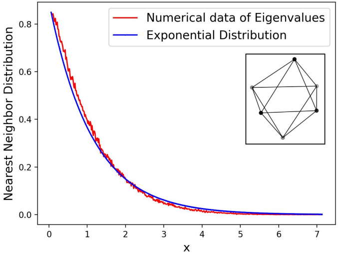

The first figure shows the (incommensurate) *cube* graph with the R coupling; as we know, in this situation vertices of *degree three* are asymptotically decoupled at high energies.

In the other we have an octahedron but the coupling matrix is changed to $U = \mathrm{e}^{i\mu}R$ with $\mu = 0.01$; as a result -1 is not an eigenvalue of U.

In both cases the eigenvalue spacing distribution is obviously *Poissonian*.

Asymptotically disconnected edges

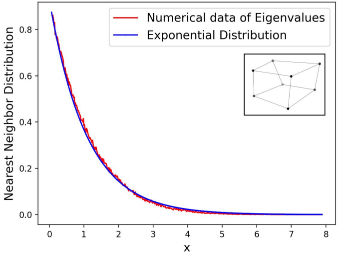

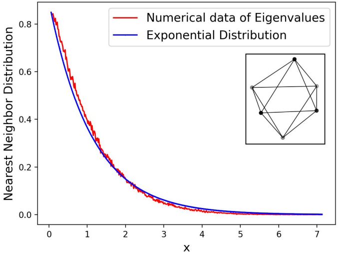

The first figure shows the (incommensurate) *cube* graph with the R coupling; as we know, in this situation vertices of *degree three* are asymptotically decoupled at high energies.

In the other we have an octahedron but the coupling matrix is changed to $U = \mathrm{e}^{i\mu} R$ with $\mu = 0.01$; as a result -1 is not an eigenvalue of U.

In both cases the eigenvalue spacing distribution is obviously *Poissonian*.

Let us look next why the GOE emerges for the R-coupled octahedron.

The time asymmetry is energy dependent

We have seen that time reversal is associated with *transposition of U* and, *mutatis mutandis*, with transposition of the scattering matrix.

The time asymmetry is energy dependent

We have seen that time reversal is associated with *transposition of U* and, *mutatis mutandis*, with transposition of the scattering matrix.

The natural measure of time-reversal invariance violation this expresses how much the S-matrix differs from its transpose; we define

$$\mathcal{M}(k) := \|S(k) - S(k)^T\|;$$

from the unitarity of $S(k)$ and triangle inequality the norm cannot exceed two. Using again $\eta := \frac{1-k}{1+k}$ we see that matrix elements of $S(k) - S(k)^T$ at a vertex of degree n are

$$M_{ij}(k) = \frac{1-\eta^2}{1-\eta^n} \left\{\eta^{(j-i-1)(\mathrm{mod}(n))} - \eta^{(i-j-1)(\mathrm{mod}(n))}\right\}.$$

The time asymmetry is energy dependent

We have seen that time reversal is associated with *transposition of U* and, *mutatis mutandis*, with transposition of the scattering matrix.

The natural measure of time-reversal invariance violation this expresses how much the S-matrix differs from its transpose; we define

$$\mathcal{M}(k) := \|S(k) - S(k)^T\|;$$

from the unitarity of $S(k)$ and triangle inequality the norm cannot exceed two. Using again $\eta := \frac{1-k}{1+k}$ we see that matrix elements of $S(k) - S(k)^T$ at a vertex of degree n are

$$M_{ij}(k) = \frac{1-\eta^2}{1-\eta^n}\left\{\eta^{(j-i-1)(\mathrm{mod}(n))} - \eta^{(i-j-1)(\mathrm{mod}(n))}\right\}.$$

This matrix is circulant, apart from the overall prefactor being generated by the vector $(c_0, c_1, \dots, c_{n-1})$ in which $c_0 = 0$ and $c_j = \eta^{j-1} - \eta^{n-j-1}$ for $j = 1, \dots, n-1$; its eigenvalues, again without the prefactor, are

$$\lambda_k(\eta) = \sum_{j=1}^{n-1} \left(\eta^{j-1} - \eta^{n-j-1}\right)\omega^{jk}, \quad k = 0, \dots, n-1,$$

Time-reversal asymmetry measure

Being primarily interested in the high-energy behavior of $\mathcal{M}_n(k)$, we must distinguish even and odd values of n. The prefactor $\frac{1-\eta^2}{1-\eta^n}$ equals

$$P_{2m}(\eta) = \frac{1}{1+\eta^2+\cdots+\eta^{2m-2}}\,, \quad P_{2m+1}(\eta) = \frac{1+\eta}{1+\eta+\cdots+\eta^{2m}},$$

which implies

$$P_{2m}(k) = \frac{1}{m} + \mathcal{O}(k^{-1}) \quad \text{and} \quad P_{2m+1}(\eta) = \frac{2}{k} + \mathcal{O}(k^{-2})$$

as $k \to \infty$. On the other hand, putting $\eta = -1+\delta$ we get the following asymptotic expansion,

$$\lambda_k(\eta) = \begin{cases} 2i\delta \sum_{j=1}^{(n-2)/2} (-1)^{j+1}(n-2j) \sin\frac{2\pi kj}{n} + \mathcal{O}(\delta^2) & \ldots\ n \text{ even} \\ 4i \sum_{j=1}^{(n-1)/2} (-1)^{j+1} \sin\frac{2\pi kj}{n} + \mathcal{O}(\delta) & \ldots\ n \text{ odd} \end{cases}$$

which allows us to find the norm of the matrix: it equals the maximum modulus of its eigenvalues.

Time-reversal asymmetry measure

Using now $\eta = -1 + 2k^{-1} + \mathcal{O}(k^{-2})$, we conclude that $\mathcal{M}_n(k) = \mathcal{O}(k^{-1})$ holds as $k \to \infty$ for any natural $n \geq 3$ for *both even and odd values of n*.

Time-reversal asymmetry measure

Using now $\eta = -1 + 2k^{-1} + \mathcal{O}(k^{-2})$, we conclude that $\mathcal{M}_n(k) = \mathcal{O}(k^{-1})$ holds as $k \to \infty$ for any natural $n \geq 3$ for *both even and odd values of n*.

In the same way one can check that $\mathcal{M}_n(k) = \mathcal{O}(k)$ as $k \to 0$.

Time-reversal asymmetry measure

Using now $\eta = -1 + 2k^{-1} + \mathcal{O}(k^{-2})$, we conclude that $\mathcal{M}_n(k) = \mathcal{O}(k^{-1})$ holds as $k \to \infty$ for any natural $n \geq 3$ for *both even and odd values of n*.

In the same way one can check that $\mathcal{M}_n(k) = \mathcal{O}(k)$ as $k \to 0$.

For low values of n it is easy to evaluate the non-invariance measure explicitly. In particular, the eigenvalues are $\{0, \pm\sqrt{3}i(1-\eta)\}$ and $\{0, 0, \pm 2i(1-\eta^2)\}$ for $n = 3, 4$, respectively, which yields

$$\mathcal{M}_3(k) = \frac{4k\sqrt{3}}{3+k^2} \quad \text{and} \quad \mathcal{M}_4(k) = \frac{4k}{1+k^2}.$$

The first relation shows that $\mathcal{M}_3(k)$ saturates the unitarity bound $\mathcal{M}(k) \leq 2$ at $k = \sqrt{3}$, while $\mathcal{M}_4(k)$ does the same at $k = 1$.

Time-reversal asymmetry measure

Using now $\eta = -1 + 2k^{-1} + \mathcal{O}(k^{-2})$, we conclude that $\mathcal{M}_n(k) = \mathcal{O}(k^{-1})$ holds as $k \to \infty$ for any natural $n \geq 3$ for *both even and odd values of n*.

In the same way one can check that $\mathcal{M}_n(k) = \mathcal{O}(k)$ as $k \to 0$.

For low values of n it is easy to evaluate the non-invariance measure explicitly. In particular, the eigenvalues are $\{0, \pm\sqrt{3}i(1-\eta)\}$ and $\{0, 0, \pm 2i(1-\eta^2)\}$ for $n = 3, 4$, respectively, which yields

$$\mathcal{M}_3(k) = \frac{4k\sqrt{3}}{3+k^2} \quad \text{and} \quad \mathcal{M}_4(k) = \frac{4k}{1+k^2}.$$

The first relation shows that $\mathcal{M}_3(k)$ saturates the unitarity bound $\mathcal{M}(k) \leq 2$ at $k = \sqrt{3}$, while $\mathcal{M}_4(k)$ does the same at $k = 1$.

Consequently, the time reversal asymmetry *asymptotically disappears*: we have $\lim_{k\to\infty} S_{ij} = -\frac{2}{n}(-1)^{i+j} + \delta_{ij}$ which differs from its Kirchhoff counterpart only by sign on the diagonal and the 'even' off-diagonals.

An alternative way to describe the form factor

A way to express the spectral condition for a finite graph of E edges is $\det\left[I - \mathbf{U}(k)\right] = 0$, where $\mathbf{U}(k) = \mathrm{e}^{ikL}\mathbf{S}(k)$ with L being the *total length* of the graph and $\mathbf{S}(k)$ the $2E \times 2E$ the unitary *global scattering matrix* (in contrast to $n \times n$ scattering matrix at a vertex of degree n)

An alternative way to describe the form factor

A way to express the spectral condition for a finite graph of E edges is $\det\left[I - \mathbf{U}(k)\right] = 0$, where $\mathbf{U}(k) = \mathrm{e}^{ikL}\mathbf{S}(k)$ with L being the *total length* of the graph and $\mathbf{S}(k)$ the $2E \times 2E$ the unitary *global scattering matrix* (in contrast to $n \times n$ scattering matrix at a vertex of degree n)

One can then express the form factor using eigenphases of the operator $\mathbf{U}(k)$, specifically at the *discrete times* $\tau \in \frac{1}{2E}\mathbb{N}$ one has

$$K_{\mathbf{U}}(\tau) = \frac{1}{2E} \lim_{\Lambda\to\infty} \frac{1}{2\Lambda} \int_{-\Lambda}^{\Lambda} \left|\mathrm{tr}(\mathbf{U}(k))^{2E\tau}\right|^2 \mathrm{d}k.$$

G. Berkolaiko: Form factor expansion for large graphs: a diagrammatic approach, in *Quantum graphs and their applications*, Contempotary Math. 415, AMS, Providence, RI, 2006; pp. 25–49.

An alternative way to describe the form factor

A way to express the spectral condition for a finite graph of E edges is $\det\left[I - \mathbf{U}(k)\right] = 0$, where $\mathbf{U}(k) = \mathrm{e}^{ikL}\mathbf{S}(k)$ with L being the *total length* of the graph and $\mathbf{S}(k)$ the $2E \times 2E$ the unitary *global scattering matrix* (in contrast to $n \times n$ scattering matrix at a vertex of degree n)

One can then express the form factor using eigenphases of the operator $\mathbf{U}(k)$, specifically at the *discrete times* $\tau \in \frac{1}{2E}\mathbb{N}$ one has

$$K_{\mathbf{U}}(\tau) = \frac{1}{2E} \lim_{\Lambda\to\infty} \frac{1}{2\Lambda} \int_{-\Lambda}^{\Lambda} \left|\mathrm{tr}(\mathbf{U}(k))^{2E\tau}\right|^2 \mathrm{d}k.$$

G. Berkolaiko: Form factor expansion for large graphs: a diagrammatic approach, in *Quantum graphs and their applications*, Contempotary Math. 415, AMS, Providence, RI, 2006; pp. 25–49.

Using the *asymptotic S-matrix* and expanding $\mathrm{tr}(\mathbf{U}(k))^{2E\tau}$ for $2E\tau \in \mathbb{N}$ as a sum of products and performing the integral we get the formula

$$K_{\mathbf{U}}(\tau) = \frac{1}{2E} \sum_{p,q} \frac{(2E\tau)^2}{r_p r_q} A_p A_q^* \delta_{L_p,L_q}.$$

An alternative way to describe the form factor

The sum runs over pairs of *periodic orbits* p consisting of $2E\tau$ edges and having length L_p; the *overall scattering amplitude* on p is denoted A_p. Some orbits may be a repetition of shorter ones with the *repetition number* r_p

An alternative way to describe the form factor

The sum runs over pairs of *periodic orbits* p consisting of $2E\tau$ edges and having length L_p; the *overall scattering amplitude* on p is denoted A_p. Some orbits may be a repetition of shorter ones with the *repetition number* r_p. As an example, we show *complete graphs* K_7 and K_9.

An alternative way to describe the form factor

The sum runs over pairs of *periodic orbits* p consisting of $2E\tau$ edges and having length L_p; the *overall scattering amplitude* on p is denoted A_p. Some orbits may be a repetition of shorter ones with the *repetition number* r_p. As an example, we show *complete graphs* K_7 and K_9.

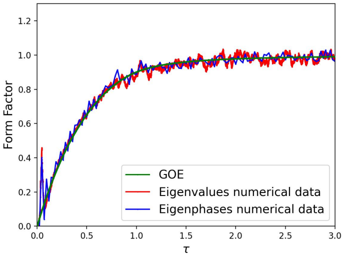

An alternative way to describe the form factor

The sum runs over pairs of *periodic orbits* p consisting of $2E\tau$ edges and having length L_p; the *overall scattering amplitude* on p is denoted A_p. Some orbits may be a repetition of shorter ones with the *repetition number* r_p. As an example, we show *complete graphs* K_7 and K_9.

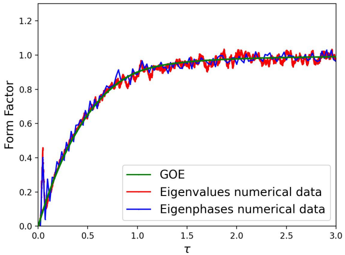

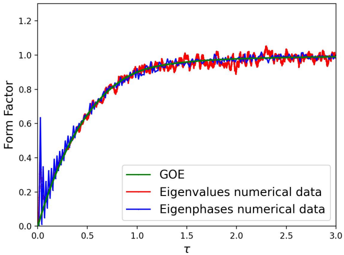

An alternative way to describe the form factor

The sum runs over pairs of *periodic orbits* p consisting of $2E\tau$ edges and having length L_p; the *overall scattering amplitude* on p is denoted A_p. Some orbits may be a repetition of shorter ones with the *repetition number* r_p. As an example, we show *complete graphs* K_7 and K_9.

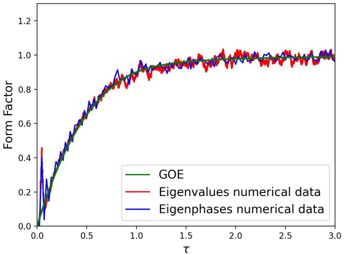

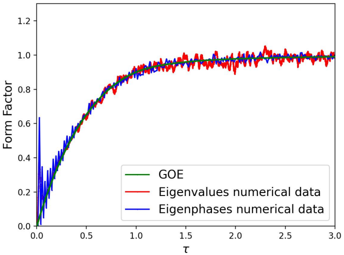

We see that both types of data fit with the GOE form factor

$$K(\tau) = \begin{cases} 2\tau - \tau \ln(1+2\tau) & \ldots \quad \tau \leq 1 \\ 2 - \tau \ln\left(\frac{2\tau+1}{2\tau-1}\right) & \ldots \quad \tau \geq 1 \end{cases} .$$

The peak at half the Heisenberg time

As we saw, the octahedron form factor has at $\tau = \frac{1}{2}$ a peak much higher than its GOE prediction, $K_{\mathrm{GOE}}(\frac{1}{2}) = 1 - \frac{1}{2}\ln 2$, and the same happens if we replace the R coupling by the Kirchhoff one:

The peak at half the Heisenberg time

As we saw, the octahedron form factor has at $\tau = \frac{1}{2}$ a peak much higher than its GOE prediction, $K_{\mathrm{GOE}}(\frac{1}{2}) = 1 - \frac{1}{2}\ln 2$, and the same happens if we replace the R coupling by the Kirchhoff one:

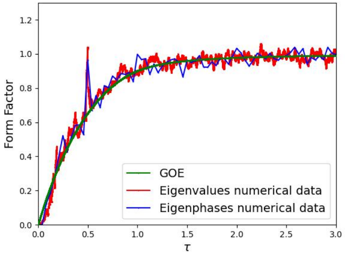

The peak at half the Heisenberg time

As we saw, the octahedron form factor has at $\tau = \frac{1}{2}$ a peak much higher than its GOE prediction, $K_{\mathrm{GOE}}(\frac{1}{2}) = 1 - \frac{1}{2}\ln 2$, and the same happens if we replace the R coupling by the Kirchhoff one:

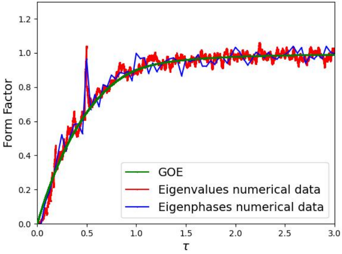

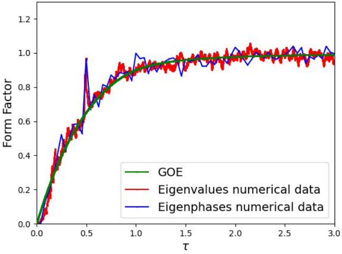

The peak at half the Heisenberg time

As we saw, the octahedron form factor has at $\tau = \frac{1}{2}$ a peak much higher than its GOE prediction, $K_{\mathrm{GOE}}(\frac{1}{2}) = 1 - \frac{1}{2}\ln 2$, and the same happens if we replace the R coupling by the Kirchhoff one:

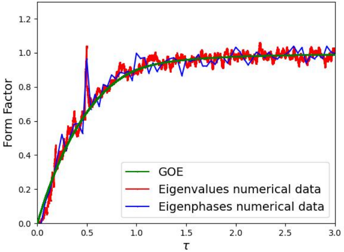

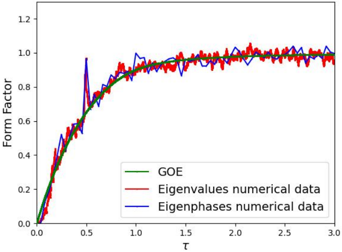

To get an understanding of the effect, we employ the above formula and estimate the contribution to the form factor coming from *periodic orbits* of length $2E\tau = E$. This requires a laborious combinatorics of which we present here only the results.

The peak at half the Heisenberg time

We focus on *Eulerian cycles*: the length of each Eulerian orbit on an *n-regular graph* Γ equals the total length of the graph, $L_p = L_q$ and $r_p = r_q = 1$, hence their contribution is $\frac{1}{2}E\sum_{p,q \text{ Eulerian}} A_p A_q^*$.

The peak at half the Heisenberg time

We focus on *Eulerian cycles*: the length of each Eulerian orbit on an *n-regular graph* Γ equals the total length of the graph, $L_p = L_q$ and $r_p = r_q = 1$, hence their contribution is $\frac{1}{2}E\sum_{p,q \text{ Eulerian}} A_p A_q^*$.

The amplitude A_p for an Eulerian cycle p is a product of transmissions amplitudes $S_{ij} = -\frac{2}{n}(-1)^{i+j}$ at vertices of the path. The contribution of each vertex to the product is $\left(\frac{2}{n}\right)^{n/2}$, and therefore

$$K_{\text{Euler}}(\tau) = \frac{1}{2}E\left(\frac{2}{n}\right)^{2E}\left(N_{\text{Euler}}(\Gamma)\right)^2.$$

The peak at half the Heisenberg time

We focus on *Eulerian cycles*: the length of each Eulerian orbit on an *n-regular graph* Γ equals the total length of the graph, $L_p = L_q$ and $r_p = r_q = 1$, hence their contribution is $\frac{1}{2}E\sum_{p,q \text{ Eulerian}} A_p A_q^*$.

The amplitude A_p for an Eulerian cycle p is a product of transmissions amplitudes $S_{ij} = -\frac{2}{n}(-1)^{i+j}$ at vertices of the path. The contribution of each vertex to the product is $\left(\frac{2}{n}\right)^{n/2}$, and therefore

$$K_{\mathrm{Euler}}(\tau) = \frac{1}{2}E\left(\frac{2}{n}\right)^{2E}\left(N_{\mathrm{Euler}}(\Gamma)\right)^2.$$

For a general Γ finding $N_{\mathrm{Euler}}(\Gamma)$ is a non-polynomial problem, for octahedron we have $N_{\mathrm{Euler}}(\Gamma_8) = 744$ so $\frac{1}{2}E\sum_{p,q \text{ Eulerian}} A_p A_q^* \approx 0.198$.

The peak at half the Heisenberg time

We focus on *Eulerian cycles*: the length of each Eulerian orbit on an *n-regular graph* Γ equals the total length of the graph, $L_p = L_q$ and $r_p = r_q = 1$, hence their contribution is $\frac{1}{2}E\sum_{p,q\ \mathrm{Eulerian}} A_p A_q^*$.

The amplitude A_p for an Eulerian cycle p is a product of transmissions amplitudes $S_{ij} = -\frac{2}{n}(-1)^{i+j}$ at vertices of the path. The contribution of each vertex to the product is $\left(\frac{2}{n}\right)^{n/2}$, and therefore

$$K_{\mathrm{Euler}}(\tau) = \frac{1}{2}E\left(\frac{2}{n}\right)^{2E}\left(N_{\mathrm{Euler}}(\Gamma)\right)^2.$$

For a general Γ finding $N_{\mathrm{Euler}}(\Gamma)$ is a non-polynomial problem, for octahedron we have $N_{\mathrm{Euler}}(\Gamma_8) = 744$ so $\frac{1}{2}E\sum_{p,q\ \mathrm{Eulerian}} A_p A_q^* \approx 0.198$.

Comparing $K_{\mathrm{GOE}}(\frac{1}{2}) \approx 0.6534$ with $K_{\mathbf{U}}(\frac{1}{2}) \approx 0.9335 \pm 0.02$ we see that Eulerian paths account for more than 70% of this mismatch.

The peak at half the Heisenberg time

We focus on *Eulerian cycles*: the length of each Eulerian orbit on an *n-regular graph* Γ equals the total length of the graph, $L_p = L_q$ and $r_p = r_q = 1$, hence their contribution is $\frac{1}{2}E\sum_{p,q \text{ Eulerian}} A_p A_q^*$.

The amplitude A_p for an Eulerian cycle p is a product of transmissions amplitudes $S_{ij} = -\frac{2}{n}(-1)^{i+j}$ at vertices of the path. The contribution of each vertex to the product is $\left(\frac{2}{n}\right)^{n/2}$, and therefore

$$K_{\mathrm{Euler}}(\tau) = \frac{1}{2}E\left(\frac{2}{n}\right)^{2E}\left(N_{\mathrm{Euler}}(\Gamma)\right)^2.$$

For a general Γ finding $N_{\mathrm{Euler}}(\Gamma)$ is a non-polynomial problem, for octahedron we have $N_{\mathrm{Euler}}(\Gamma_8) = 744$ so $\frac{1}{2}E\sum_{p,q \text{ Eulerian}} A_p A_q^* \approx 0.198$.

Comparing $K_{\mathrm{GOE}}(\frac{1}{2}) \approx 0.6534$ with $K_{\mathbf{U}}(\frac{1}{2}) \approx 0.9335 \pm 0.02$ we see that Eulerian paths account for more than 70% of this mismatch.

They are a tiny part of all periodic orbits of length 12 whose number is about 1.4×10^6. Their significance is due to *constructive interference:* for Eulerian cycles all the contributions to the sum are *positive*.

Other graphs with peaks

The effect is not restricted to the R coupling. We have seen the same in case of octahedron with the *Kirchhoff coupling* which is natural as the scattering matrices differ by sign only which plays no role

Other graphs with peaks

The effect is not restricted to the R coupling. We have seen the same in case of octahedron with the *Kirchhoff coupling* which is natural as the scattering matrices differ by sign only which plays no role. Note that the effect may exist even if the vertex coupling is *time reversal invariant*, now with the 'correct' vertex scattering matrix.

Other graphs with peaks

The effect is not restricted to the R coupling. We have seen the same in case of octahedron with the *Kirchhoff coupling* which is natural as the scattering matrices differ by sign only which plays no role. Note that the effect may exist even if the vertex coupling is *time reversal invariant*, now with the 'correct' vertex scattering matrix.

This is not all; for the complete graph K_5, e.g., we have peaks again with the Eulerian contribution equal to $\frac{1}{2}E\sum_{p,q \text{ Eulerian}} A_p A_q^* \approx 0.332$

Other graphs with peaks

The effect is not restricted to the R coupling. We have seen the same in case of octahedron with the *Kirchhoff coupling* which is natural as the scattering matrices differ by sign only which plays no role. Note that the effect may exist even if the vertex coupling is *time reversal invariant*, now with the 'correct' vertex scattering matrix.

This is not all; for the complete graph K_5, e.g., we have peaks again with the Eulerian contribution equal to $\frac{1}{2}E\sum_{p,q \text{ Eulerian}} A_p A_q^* \approx 0.332$

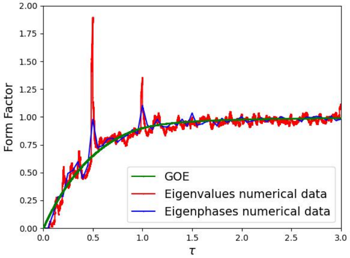

Other graphs with peaks

The effect is not restricted to the R coupling. We have seen the same in case of octahedron with the *Kirchhoff coupling* which is natural as the scattering matrices differ by sign only which plays no role. Note that the effect may exist even if the vertex coupling is *time reversal invariant*, now with the 'correct' vertex scattering matrix.

This is not all; for the complete graph K_5, e.g., we have peaks again with the Eulerian contribution equal to $\frac{1}{2}E\sum_{p,q \text{ Eulerian}} A_p A_q^* \approx 0.332$

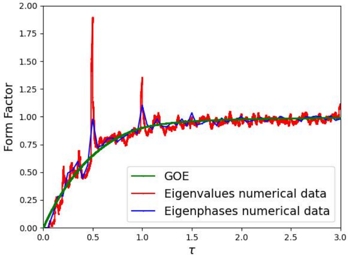

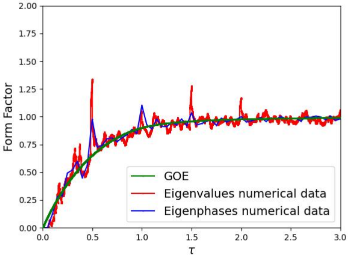

Other graphs with peaks

The effect is not restricted to the R coupling. We have seen the same in case of octahedron with the *Kirchhoff coupling* which is natural as the scattering matrices differ by sign only which plays no role. Note that the effect may exist even if the vertex coupling is *time reversal invariant*, now with the ‘correct’ vertex scattering matrix.

This is not all; for the complete graph K_5, e.g., we have peaks again with the Eulerian contribution equal to $\frac{1}{2}E\sum_{p,q \text{ Eulerian}} A_p A_q^* \approx 0.332$

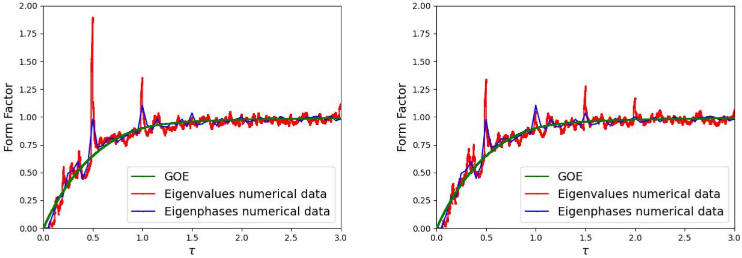

Moreover, there are smaller peaks at other half-integer values, especially in the Kirchhoff case.

However, it is not always the case

It is no surprise that one finds no such peaks in *non-Eulerian graphs* such as complete graphs with even number of vertices.

However, it is not always the case

It is no surprise that one finds no such peaks in *non-Eulerian graphs* such as complete graphs with even number of vertices.

However, even in Eulerian graphs the effect *not necessarily present*; recall the plots for K_7 and K_9 shown above. The point is that the contribution from Eulerian cycles does not vanish but becomes insignificant:

However, it is not always the case

It is no surprise that one finds no such peaks in *non-Eulerian graphs* such as complete graphs with even number of vertices.

However, even in Eulerian graphs the effect *not necessarily present*; recall the plots for K_7 and K_9 shown above. The point is that the contribution from Eulerian cycles does not vanish but becomes insignificant:

For K_7 with the values $E = 21$, $n = 6$ and $N_{\mathrm{Euler}}(K_7) = 129976320$, their contribution to the peak is about 0.00162 while $K_{\mathrm{GOE}}(\frac{1}{2}) \approx 0.6534$, so no peak at $\tau = \frac{1}{2}$ is seen in this case.

However, it is not always the case

It is no surprise that one finds no such peaks in *non-Eulerian graphs* such as complete graphs with even number of vertices.

However, even in Eulerian graphs the effect *not necessarily present*; recall the plots for K_7 and K_9 shown above. The point is that the contribution from Eulerian cycles does not vanish but becomes insignificant:

For K_7 with the values $E = 21$, $n = 6$ and $N_{\mathrm{Euler}}(K_7) = 129976320$, their contribution to the peak is about 0.00162 while $K_{\mathrm{GOE}}(\frac{1}{2}) \approx 0.6534$, so no peak at $\tau = \frac{1}{2}$ is seen in this case.

Similarly, for K_9 with $N_{\mathrm{Euler}}(K_9) = 911520057021235200$, $E = 36$ and $n = 8$, the contribution amounts to the negligible 6.7×10^{-7}; one can check that it tends to zero for K_{2n+1} as $n \to \infty$.

However, it is not always the case

It is no surprise that one finds no such peaks in *non-Eulerian graphs* such as complete graphs with even number of vertices.

However, even in Eulerian graphs the effect *not necessarily present*; recall the plots for K_7 and K_9 shown above. The point is that the contribution from Eulerian cycles does not vanish but becomes insignificant:

For K_7 with the values $E = 21$, $n = 6$ and $N_{\mathrm{Euler}}(K_7) = 129976320$, their contribution to the peak is about 0.00162 while $K_{\mathrm{GOE}}(\frac{1}{2}) \approx 0.6534$, so no peak at $\tau = \frac{1}{2}$ is seen in this case.

Similarly, for K_9 with $N_{\mathrm{Euler}}(K_9) = 911520057021235200$, $E = 36$ and $n = 8$, the contribution amounts to the negligible 6.7×10^{-7}; one can check that it tends to zero for K_{2n+1} as $n \to \infty$.

In conclusion, there may be deviation from the universal behavior of chaotic quantum graphs coming both from the *time reversal asymmetry* and the *smallness* of the graph in combination with its *topology*.

It remains to say

It remains to say

Thank you for your attention!